scientific reports

Check for updates

OPEN

Bioinspired multifunctional silver nanoparticles by *Smilax Chenensis* and their enhanced biomedical and catalytic applications

Susmila Aparna Gaddam[1], Venkata Subbaiah Kotakadi[2]✉, Rajasekar Allagadda[3], Vasavi T.[4], Siva Gayathri Velakanti[1], Srilakshmi Samanchi[5], Devaraju Thangellamudi[6], Hema Masarapu[1], Uma Maheswari P[4], Appa Rao Ch[3] & Enyew Amare Zereffa[7]✉

Currently, Nano-materials have been explored for their abundant biomedical applications. In the present study the green synthesized (SC-AgNPs) by root extract of *Smilax Chenensis* have been characterized by UV–visible spectroscopy revealed SPR peak at 432 nm and FT-IR data reveals that the bioactive components of root extract have been actively involved in the reduction and stabilization of SC-AgNPs. TEM and AFM results revealed that SC-AgNPs were roughly spherical in shape. Further, the particle size of SC-AgNPs was also carried out by Dynamic Light Scattering method by aqueous colloidal solution and the results reveals that the SC-AgNPs are poly-dispersed in nature with an average size 45.6 nm with a Z average of 39.5 nm. The stability of colloidal SC-AgNPs was further confirmed by negative zeta potential value of − 21.0 mV. The SC-AgNPs showed good antibacterial activity against both gram –ve and gram + ve bacteria, whereas, SC-AgNPs coupled with antibiotic reveals excellent and enhanced antibacterial activity. The gram –ve *E.coli* and gram + ve *S.aureus* revealed highest zone of inhibition when compared to other two bacterial species. So, SC-AgNPs coupled with antibiotics can be excellent alternative to treat antibiotic resistant bacteria. The SC-AgNPs also reveals excellent antioxidant activity among them DPPH method revealed superior activity with an IC_{50} value76.22. The SC-AgNPs also reveals superior anticancer activity against MDA-MB-231 with IC_{50} value of 33.98 µg/mL and photo-catalytic activity the optical density of reduced from 1.861 to 0.135 OD within 30 min. The green SC-AgNPs detected to have multiple therapeutic applications.

Keywords *Smilax Chenensis*, Root extract, Silver nanoparticles, Spectral analysis, Antibacterial activity, Antioxidant activity, In-vitro cytotoxic studies, Dye degradation

Nanotechnology is an advanced scientific branch which deals materials at the atomic level, preferably between 1 and 100 nm, by means of various physical, chemical, and biological approaches. These nanomaterials have different physical and chemical properties have emerged with advancement in Nanotechnology. These nanomaterials have been explored for abundant biomedical applications due their nanoscale size. Moreover the developments in the area of metallic nanoparticles (NPs) synthesis and research have show the way to advancements in personalized healthcare, diagnostics, and therapies[1–5].These metallic NPs have fascinated scientists for more than four decades, at the present they were widely used in engineering and medical fields. The metals like Ag, Cu, Au, Pt, Zn, Mg, etc., and their metal oxides have been shown significant beneficial advantage in the field of medicine. These NPs have been employed in biosensors, diagnostic imaging, and drug delivery applications[6–10]. Particularly, metal NPs like silver and gold have stolen the limelight and have been subject to extensive research due to their unique characteristics such as their size and high surface area. Especially the synthesis of AgNPs and AuNPs are usually synthesized using hazardous chemicals, which affect the environment

[1]Department of Virology, Sri Venkateswara University, Tirupati, Andhra Pradesh 517502, India. [2]DST-PURSE Centre, Sri Venkateswara University, Tirupati, Andhra Pradesh 517502, India. [3]Department of Biochemistry, Sri Venkateswara University, Tirupati, Andhra Pradesh 517502, India. [4]Department of Applied Microbiology, SPMVV(Women's University), Tirupati, Andhra Pradesh 517502, India. [5]Department of Biotechnology, SPMVV(Women's University), Tirupati, Andhra Pradesh 517502, India. [6]Department of EEE, Mohan Babu University, Tirupati, Andhra Pradesh 517502, India. [7]Department of Applied Chemistry, School of Applied Natural Sciences, Adama Science and Technology University, Adama, Ethiopia. ✉email: kotakadi72@gmail.com; eneyew.amare@astu.edu.et

and human health. Therefore it's highly necessary to initiate the development of eco-friendly techniques to rise to the green synthesis methodology. This necessitated the steps forward towards environment-friendly techniques and gave rise to the 'green synthesis' methods[11–16]. Plant-based biological molecules in the form of extracts are the backbone of plant-mediated production of NPs, which outperforms conventional chemical techniques. In the current scenario, several researchers are widely using the plant-based natural molecules or bioactive components in the form of aqueous extracts are the major backbone of plant-mediated green synthesis of metal nanoparticles, which is replaced and outperforms regular conventional chemical and physical methods. These metallic nanoparticles exhibit novel therapeutic and characteristics functions such as antibacterial, antioxidant, antitumor and wound repair etc.[17–20]. Because of these outstanding benefits in biomedical field, green synthesis of plant-based NPs by eco-friendly techniques have shown remarkable advancements. At the same they can be easily engineered, to controllable size and shape with improved health benefits and also their fascinating applications related to several industries[21–26].

Presently, cancer is the major problem throughout the world. It is a disease in which the body cells grow without control and spread to other parts of the body. Human body is made up of trillions of cells; they grow and multiply by a process called cell division when the body needs them. Whereas in case of cancer, the orderly process of cell division break down and the cells are damaged and multiply abnormally and form tumors, in other way lumps of tissue, which can be cancerous or benign (non cancerous). The current statistics on cancer reveals, it is a leading cause of deaths worldwide. One in six was affected by cancer leads to 10 million deaths in 2020 (WHO, 2022)[27]. The most common cancers are breast cancer, lung cancer, colon cancer and rectum cancer and prostate cancers. The main cause of cancer deaths are due to tobacco use, alcohol consumption, low fruit and vegetable intake and high body mass index and finally lack of physical activity. If detected early it can be treated effectively. Breast cancer is the one of leading cancer currently, which causes abnormal breast cells grow out of control and form tumors, it can be fatal if undetected. There were more than 2.3 million women diagnosed with breast cancer in the year 2020 (WHO, 2022)[27] and 685,000 deaths globally. Enthrallingly more than 7.8 million women were alive, who were diagnosed with breast cancer in the last 5 years, making the breast cancer as a primary cancer in the world. The main treatments for breast cancer treatment are chemotherapy and radiation therapy which have several side effects[27]. Scientists have been working on alternative methods to overcome this problem. Nanotechnology and green synthesis of metal nanoparticles have opened new avenues to the above problem. Green synthesized silver nanoparticles have been widely used to target breast cancer as a future alternative therapy[28–38]. Several metal nanoparticles have been used to target various cancers by site directed targeted drug delivery on cancer tissue alone in the body, which can avoid the damage of surrounding healthy cells or organs in the human body unlike chemotherapy and radiation therapy.

Antimicrobial resistance is a new major problem facing by the present generation of the world population today. The habit of usage of high end antibiotics to various illnesses, the disease causing microorganisms has developed resistant to the antibiotics. To overcome this problem the scientific fraternities have been working since three decades. They have found that the green synthesized metal nanoparticles can be best source to overcome the prime problem. Silver nanoparticles synthesized by various plant sources have shown excellent antimicrobial properties on both pathogenic and nonpathogenic bacterial strains[39–44].

Based on the above fascinating advantages of Nanotechnology, it's applications for protection of mankind and nature with the help of using plant-based metal NPs. An interesting study was conducted at our research laboratory, green synthesis silver nanoparticles (AgNPs) by an important Ayurvedic medicinal plant namely *Smilax chineses* or *Smilax china* L. popularly known has 'Chinese root' or 'China root'. *Smilax china* L., is an important perennial climbing plant belongs to family Liliaceae. It is distributed worldwide in tropical and temperate regions of eastern Asia and North America[45]. In China the *Smilax china* L is widely reported as a medicinal plant of folk medicine, at the same time it has been reported as wonder drug, as per Indian Ayurveda. It has several health benefits and used to treat several diseases such as tumors, acute bacterial dysentery, gout, rheumatic arthritis and chronic pelvic inflammatory disease[46,47]. In addition, it is also included in the 2020 edition of the Pharmacopoeia of China[48,49]. *Smilax china* L is known as an important therapeutic plant, which is edible with medicinal value and most importantly economic value also. Depending on its pharmacological importance, there is lot of demand on these plants. So the researchers and scientists have focused to explore the opportunities and benefits of *Smilax china* L for the mankind. Firstly, they have detected the botanical and ethno-pharmacology studies of this plant. The phyto-chemical researchers have developed special interest regarding *Smilax china* L plant and have developed rapid detection and separation technology to isolate many important bioactive and biochemical components like saponins, polyphenols, flavonoids, polysaccharides, and amino acids[50,51]. These plants are also rich in its nutrients, which contains amino acids, fats, organic acids, salts and minerals etc., among them they have seven important kinds of amino acids which are highly necessary for human body, and foremost amino acid histidine for development of infants' body. The plants have remarkable edible value, the tender buds and leaves are eaten as delicious vegetables, the rhizome are used for extraction of starch and serve as raw material for brewing and finally to treat many diseases. Especially the rhizome of *Smilax china* is of high medicinal value and has a variety of pharmacological and medicinal activities such as antioxidant, anti-inflammatory, anti-tumor, anti-obesity, anti-diabetes, anti-hyperuricaemia, anti-hypertension, detoxify nicotine, promoting skin wound and barrier repair and anti-bacterial activity and other effects[52–59].

So, by keeping in view of several pharmacological properties of *Smilax china*, the current study was carryout by root extract of the plant. The silver nanoparticles were green synthesized and were characterized by using various spectroscopic methods viz. UV–visible spectroscopy, FTIR, Particle size & Zeta potential, XRD, TEM studies. The SC-AgNPs were also used to study antioxidant and antibacterial (SC-AgNPs only & SC-AgNPs coupled with Antibiotic) and in vitro anti-cancer activities were evaluated against breast cancer cell line, to discover their possible therapeutic application of SC-AgNPs.

Experimental section

Collection of plant material and chemicals and other materials

Smilax china.L., root powder (S.1.) was collected from Sri Venkateswara Ayurveda College of Pharmacy, Srinivasa mangapuram, Tirupati, Andhra Pradesh, India. We used the following chemicals and glass ware as follows: silver nitrate (Sigma–Aldrich, Munich, Germany), Nutrient agar, nutrient broth (Himedia, Mumbai, India), Potassium bromide (Sigma–Aldrich), antibiotic discs (Himedia), glassware (Borosil, Mumbai, India), and Whatman No. 1 filter paper. MDA-MB-231cell lines were procured from NCCS (Pune), DMEM(Dulbecco's Modified Eagle's Medium), 90% + 10% FBS (Foetal Bovine Serum) with 1% pen- strep solution and 5% CO_2 and 37 ℃ in a humidifying incubator.

Green synthesis of SC-AgNPs

Smilax china root extract was prepared, by taking 5 g of finely powdered roots with 150 ml Milli-Q water in a clean and sterile 250 ml conical flask and mixed thoroughly and then the mixture was heated at 70 °C for 30 min. After 30 min the root extract sample was filtered through sterile muslin cloth followed by Whatman no.1 filter paper subsequently. The filtrate was stored at 4 ℃ until further use. The diluted e extract was used to carry out the green synthesis of silver nanoparticles. To 1 mL of root extract, 4 mL of sterile Milli-Q water and 10 mL of 0.002 M Silver Nitrate solution ($AgNO_3$) were added and left at room temperature and the reaction was observed. The experiment was carried by Gaddam et al. 2021 green synthesis protocol[17]. The colorless root extract was reduced by $AgNO_3$ solution and the color of the solution changed to light brown to dark brown within 5 min after adding silver nitrate (Fig. 1b, c). The color change indicated the reduction of silver ions into elemental silver i.e. AgNPs. The previous studies also reveal that AgNPs exhibit a dark brown color in aqueous solution due to surface plasmon resonance (SPR). In the present study, the AgNPs were synthesized by *Smilax china* root extract without any external toxic chemicals. Thus, this method is popularly known "Green synthesis". The green synthesized AgNPs by root extract of *Smilax china* are named as "SC-AgNPs". The green synthesized SC-AgNPs colloidal solution was centrifuged at 15,000 rpm per 20 min, the obtained SC-AgNPs pellet was washed thrice with Milli Q water by repeating the centrifugation step to remove the unbound plant bio-molecules on the surface of the SC-AgNPs. The final SC-AgNPs pellets were dissolved in sterile Milli Q water and used for further studies like spectral characterization and biomedical applications like antibacterial, antioxidant and anticancer studies.

Spectral characterization of SC-AgNPs

Spectral analysis consists of various important spectroscopic tools for characterization of metal nanoparticles. In the current study, green synthesized SC-AgNPs were detected as soon as the colour change of reaction mixture was observed visually after 5 min. The green synthesized SC-AgNPs were immediately analyzed in Nanodrop–UV–visible spectrometer and recorded its surface Plasmon resonance (SPR) peak. The absorption spectra of SC-AgNPs was recorded by sampling 1–3 µL of sample at regular time interval at room temperature at the resolution of 1 nm between 220–750 nm (Nanodrop 8000, UV–visible spectrophotometer Thermo Scientifics, available at DST PURSE centre, Sri Venkateswara University, Tirupati). Fourier transform infrared spectroscopy (FTIR) analysis of *Smilax china* root extract and green synthesized SC-AgNPs was carried out using Bruker Tensor 27, Thermo Scientifics, USA, available at Department of Chemistry, Sri Venkateswara University, Tirupati. The FTIR study is crucial to find out which bioactive compounds are present in the root extract of *Smilax china,* and also to detect the bioactive compounds which are actively involved bio-reduction and green synthesis of SC-AgNPs. Further, the Particle size of SC-AgNPs was carried out by Dynamic light scattering (DLS) method by using Nanopartica Horiba SZ-100, Japan, available at DST PURSE centre, Sri Venkateswara University, Tirupati. It is very useful to find out the of the size distribution of green synthesized SC-AgNPs in the purified aqueous colloidal solution. Zeta potential analysis was also carried out to find out the stability of SC-AgNPs in the aqueous colloidal solution (Nanopartica Horiba SZ-100). The X-ray diffraction (XRD) analysis was also carried out to detect and understand the crystalline nature of green synthesized SC-AgNPs. The X-ray diffraction (XRD) pattern measurements of drop-coated film of SC-AgNPs on aluminum foil substrate were recorded at a wide range of Bragg angles 2 h at a scanning rate of 2 min^{-1} and carried out on a spectroscopy using Seifert Rayflex 300TT X-ray diffractometer with CuK (k = 1.542A°) radiation that was operated at a voltage of 40 kV and a current of 30 mA with CuK (k = 1.545A°) radiation. Additionally, advanced Atomic force microscopy studies on green synthesized SC-AgNPs was carried out by coating a thin film of SC-AgNPs on a sterile clean glass bits, they are air-dried prior to the analysis to detect the exact size and morphology of the SC-AgNPs (AFM-Solver Next, NT-MDT, Russia, available at DST PURSE centre, Sri Venkateswara University, Tirupati). Finally high resolution–transmission electron microscopy (HR-TEM) analysis was also carried out to find out the shape and size of green synthesized SC-AgNPs, the purified colloidal sample of SC-AgNPs was coated by adding a drop on carbon coated copper grid later the sample was dried under a mercury lamp for 5 min prior to TEM analysis. TEM analysis was carried out using High Resolution Transmission Electron Microscope 200 kV Bharathiar University, Coimbatore, Tamilnadu).

Antibacterial studies of SC-AgNPs

The antibacterial studies of green synthesized SC-AgNPs was determined against both gram negative and gram positive bacterial strains. To detect competence of SC-AgNPs, gram –ve *Escherichia coli* and *Pseudomonas aeruginosa and* gram + ve *Staphylococcus aureus* and *Bacillus megatrium* by using Agar disc-diffusion method standardized by Kotakadi et al.[39,40]. The green synthesized SC-AgNPs were loaded on 5 mm sterile Whatman No 1 filter paper discs, at different concentrations as follows 10 µg (10 mcg), 20 mcg, 30 mcg, along with standard antibiotic [amoxicillin (10 mcg)]. The zones of inhibition (ZOI) of SC-AgNPs of the above concentrations were recorded.

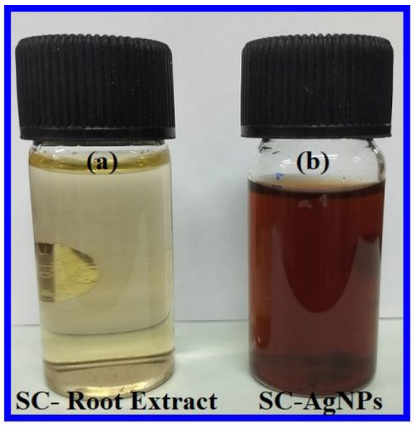

(c)

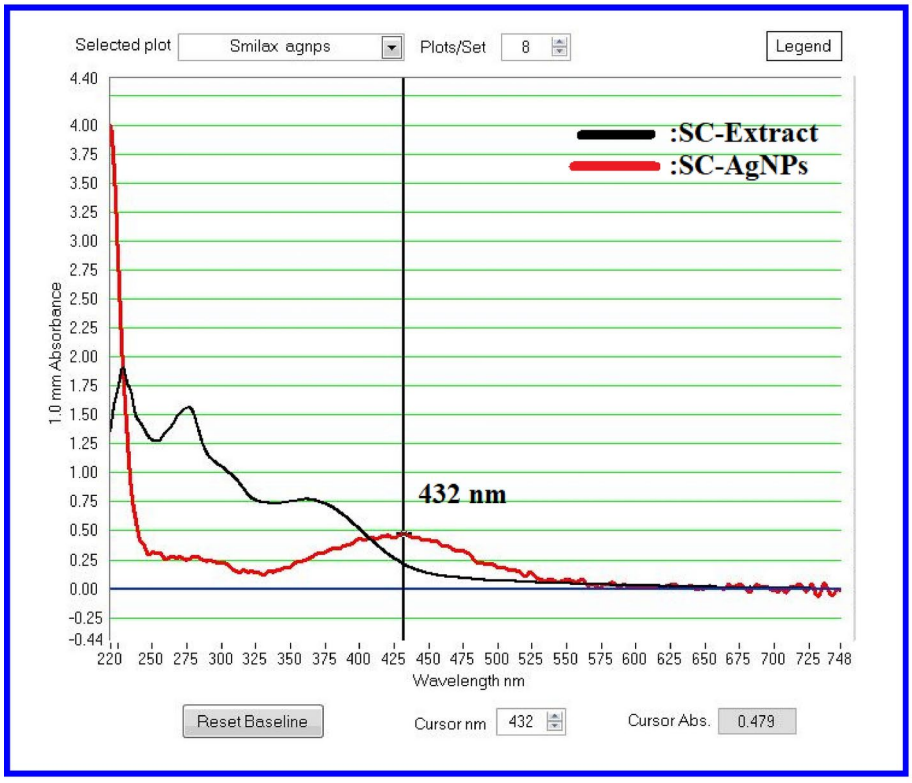

Fig. 1. (**a**) *Smilax china* L. root extract (**b**) SC-AgNPS (the reaction solution changing from light pale color to dark brown color indicates formation of AgNPs). (**c**) UV–visible spectral analysis of SC root extract and SC-AgNPs.

Antibacterial studies of SC-AgNPs coupled with antibiotic

Similarly, the antibacterial studies of green synthesized SC-AgNPs coupled with antibiotic were also determined against both gram − ve *Escherichia coli* and *Pseudomonas aeruginosa* and gram + ve bacterial strains such as *Staphylococcus aureus* and *Bacillus megatorium*, by using Agar disc-diffusion method standardized by Kotakadi et al.[39,40]. Here the antibiotic disc of Amoxicillin (10 mcg) were loaded with different concentrations of the green synthesized SC-AgNPs follows 10 µg (10 mcg), 20 mcg, 30 mcg, along with standard antibiotic amoxicillin (10 mcg). The zones of inhibition (ZOI) of SC-AgNPs coupled with antibiotic were recorded.

Free radical scavenging activity of SC-AgNPs by DPPH method

The antioxidant activity of SC-AgNPs was carried out by using 2, 2′- diphenyl-1-picrylhydrazyl (DPPH) radical scavenging assay according to the method described by Gaddam et al. and Kotakadi et al. with slight modifications[17,18]. The 2 mL of DPPH solution was added to 1 mL of methanol solution containing test samples of root extract of *Smilax china* L., and green synthesized SC-AgNPs at different concentrations of 25 µg/mL, 50 µg/mL, 75 µg/mL and 100 µg/mL. The DPPH radical scavenging activity (RSA) was measured by determining the absorbance at 517 nm, using ascorbic acid as standard and the antioxidant activity.

$$\text{RSA } (\%) = [(\text{control absorbance} - \text{sample absorbance})/(\text{control absorbance})] \times 100$$

Antioxidant activity of SC-AgNPs by NO method

The Nitric oxide scavenging activity was carried out by a tailored method of Ferreira et al.[60]. Nitric oxide radicals (NO) were generated from sodium nitroprusside. Sodium nitroprusside (1 mL of 10 mM) and 1.5 mL of phosphate buffer saline (0.2 M, pH 7.4) were added to different concentrations (25 µg/mL, 50 µg/mL, 75 µg/mL and 100 µg/mL) of the SC-AgNPs and root extract of *Smilax china* L., and incubated for 150 min at 25 ℃. The reaction mixture (1 mL) was treated with 1 mL of Griess reagent (1% sulfanilamide, 2% H_3PO_4 and 0.1% naphthylethylenediamine dihydrochloride). The absorbance of the reaction mixture was measured at 546 nm and nitric oxide scavenging activity was calculated using the equation as defined for DPPH scavenging activity.

Antioxidant activity of SC-AgNPs by H_2O_2 method

H_2O_2 scavenging ability of the *Smilax china* L., root extract and green synthesized SC-AgNPs at different concentrations of 25 µg/mL, 50 µg/mL, 75 µg/mL and 100 µg/mL, was examined according to the modified method of Pick and Mizel[61]. H_2O_2 (40 mM) solution was prepared in phosphate buffer (pH 7.4), SC-AgNPs and root extract at different concentrations of 25 µg/mL, 50 µg/mL, 75 µg/mL and 100 µg/mL in 3.4 mL phosphate buffer were added to H_2O_2 solution (0.6 mL, 40 mM). The absorbance of the reaction mixture was recorded at 230 nm and the percent of scavenging activity of H_2O_2 was determined using the equation as defined for DPPH scavenging activity.

In-vitro cytotoxic activity of SC-AgNPs on human breast adeno carcinoma cell lines

The cytotoxic activity of SC-AgNPs was assessed by MTT assay[62], (MTT = "3-(4,5-Dimethylthiazol-2-yl)-2,5-diphenyl tetrazolium bromide" assay). Principle: MTT (3-(4,5-dimethyl thiazol -2-yl)-2,5 diphenyl tetrazolium bromide)is a water soluble salt and succinate dehydrogenases of mitochondria convert it into insoluble purple formazan product. The viability of the cells is indicated by the intensity of the purple colour which can be read at 570 nm. MDA-MB-231cell lines were procured from NCCS (Pune) and routinely maintained in DMEM (Dulbecco's Modified Eagle's Medium) 90% + 10% FBS (Foetal Bovine Serum) with 1% pen- strep solution at 5% CO_2 and 37^0C in a humidifying incubator. Protocol: 1. MDA-MB-231 cells were seeded in 96-well plate and incubated in CO_2 incubator (5% CO_2 and 37 ℃). 2. After 24 h the medium was removed and fresh medium without FBS was added. 3. The purified SC-AgNPs were dissolved in 0.1% DMSO was filtered using PVDF syringe filters and added to the wells in different concentrations as follows: 10 µg/mL, 25 µg/mL, 50 µg/mL, 75 µg/mL and 100 µg/mL of SC-AgNPs and Cell Control. 4. Final volume in all wells was made equal (200µL). 5. Incubated at 37 ℃, 5% CO_2 in humidifying CO_2 incubator. 6. 20 µL of MTT solution [5 mg/mL in warm PBS was added to each well. 7. Incubation was extended for another 4 h. 8. MTT solution was removed and formazan crystals were dissolved using DMSO (for 20 min). 9. The absorbance was read at 570 nm. 10 To calculate IC_{50} value we have used MS-office Excel software. 11. Cell proliferation percentage was calculated using the following formula-

$$\text{Cell proliferation } \% = \frac{\text{OD of sample}}{\text{OD of control}} \times 100$$

Catalytic reduction of cotton blue dye degradation by SC-AgNPs

5 mg of Cotton blue dye was added to 100 mL of Milli Q distilled water used as stock solution. About 250 µl of green synthesized silver nanoparticles were added to 2.5 mL of Cotton blue dye solution. A blank was maintained without addition of silver nanoparticles SC-AgNPs. The reaction suspension was mixed well to the equilibrium of the working solution. The suspension was used to evaluate the photo-catalytic degradation of dye[84]. The absorbance spectrum of the suspension was subsequently measured at different time interval using Nanodrop-8000, UV–Vis spectrophotometer at the different wavelength 220–750 nm. Concentration of dye during degradation was calculated by the absorbance values and percentage of dye degradation was estimated. The graph of dye degradation was drawn using MS-office Excel software.

Results and discussion

Green synthesis of SC-AgNPs and UV–visible spectral analysis of SC-AgNPs

The UV–visible spectroscopy result revealed that the root extract of *Smilax china* L., has ability to convert silver nitrate solution into the ionic form Ag^+ to Ag^0. The diluted pale colour root extract reacts with 0.02 M silver nitrate solution and reduce to ionic form, confirmed by changing reaction solution to dark brown colour (Fig. 1a, b).

The surface plasmon resonance spectrum (SPR) peak of green synthesized SC-AgNPs was obtained at 432 nm (Fig. 1c). The earlier studies on green synthesis of silver nanoparticles by various plants extracts have noticed that the SPR peak intensity increase with the time intervals and concentration of $AgNO_3$ from 0.001 to 0.005 M. The earlier studies on green synthesized AgNPs also revealed similar type results using different parts of plants, like leaf extract *Argyreia nervosa*[19], *Decaschistia crotonifolia*[20]. Flower extract of *Aerva lanata*[21], leaf extract of *Britneria herbeae*[63], & bark extract of *S mahagoni*[64].

FTIR analysis of SC-AgNPs

FTIR analysis of *Smilax china* L root extract and green synthesized SC-AgNPs were shown in Fig. 2a, b. The FTIR peaks for *Smilax china* L root extract detected at 3417.26, 2906.36, 1636.22, 1406.42, 1252.03, 1153.48, 1080.14, 1027.34, 833.02, 708.17 and 579.03 cm^{-1}. Whereas the IR peaks of green synthesized SC-AgNPs were detected

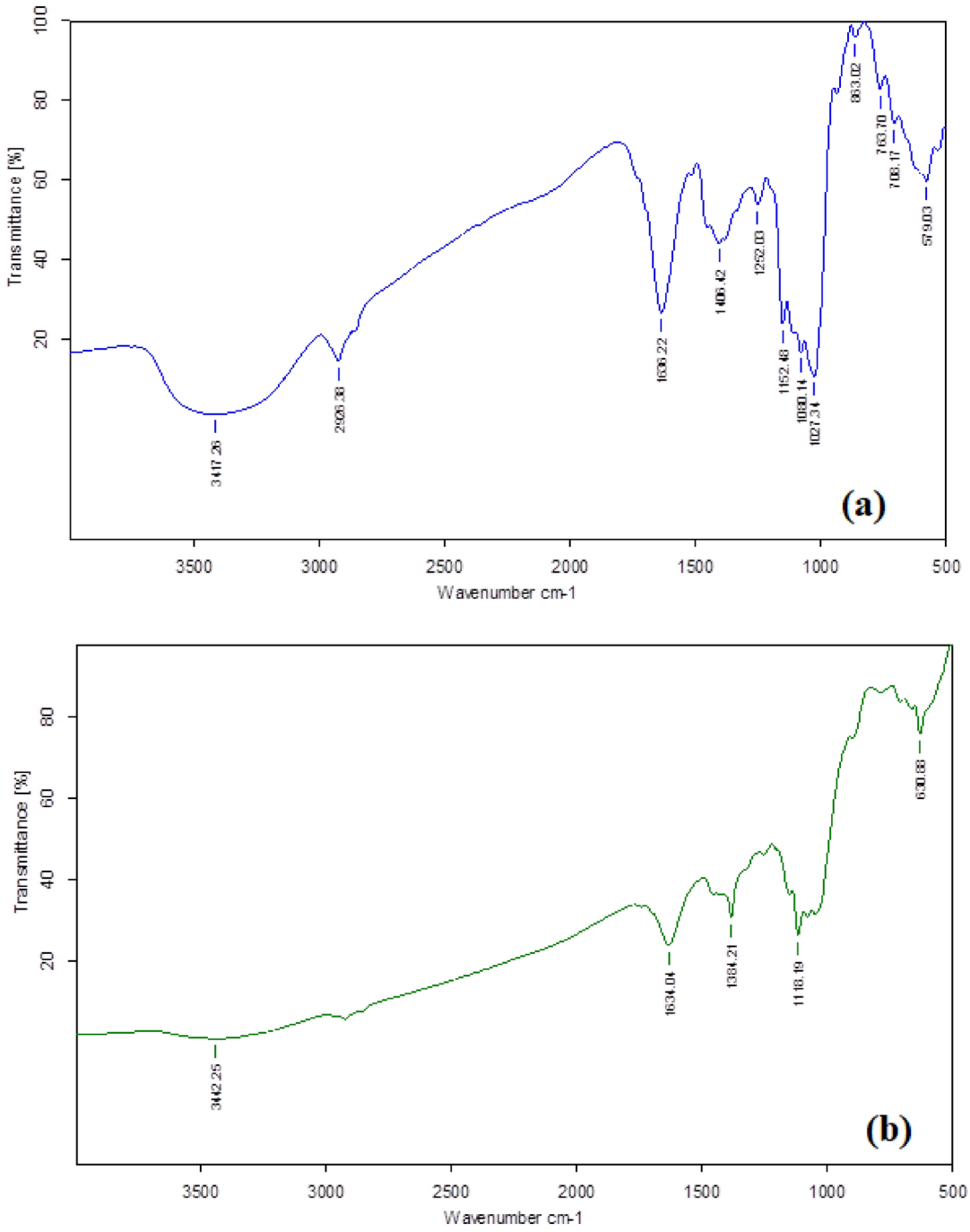

Fig. 2. (**a**) FTIR analysis of root extract of *Smilix china L.* & (**b**) FTIR analysis of green synthesized SC-AgNPs.

at 3442.25, 1634.04, 1384.21, 1118.19 and 630.88 cm^{-1} respectively, from these data it is clearly understood that the bioactive compounds present in root extract of *Smilax china* L, are responsible for bio-reduction and stabilization of SC-AgNPs. The results were analyzed and compared as follows: the strong and broad peaks of root extract and green SC-AgNPs shown in Fig. 2a, b reveals peaks at 3417.26 and 3442.25 cm^{-1} corresponds to –NH stretching in amide II and also the hydrogen-bonded hydroxyl (OH), were observed in both the root extract and SC-AgNPs. The peak at 2906.36 cm^{-1} corresponds to asymmetric stretching of C–H group and the other peaks, 1636.22, peak of root extract and 1634.04, peaks of Sc-AgNPs were identified as the characteristic peaks for the C–H, C–C, C–O stretching and the amide I group due to the carbonyl vibrational stretches in amide group linkages in proteins. The other peaks at 1406.42, and 1384.21, cm^{-1} corresponds to C–N stretching of aromatic amines. The peaks 0f. root extract at 1252.03, 1153.48, 1080.14, 1027.34 and 1384.21, 1118.19 of SC-AgNPs reveals the intense peaks at 1046 and 1043 cm^{-1} are the bands corresponding to characteristic peaks of C–OH stretching of secondary alcohols, carboxylic acids, and ester and ether groups. Finally the peaks at 833.02,

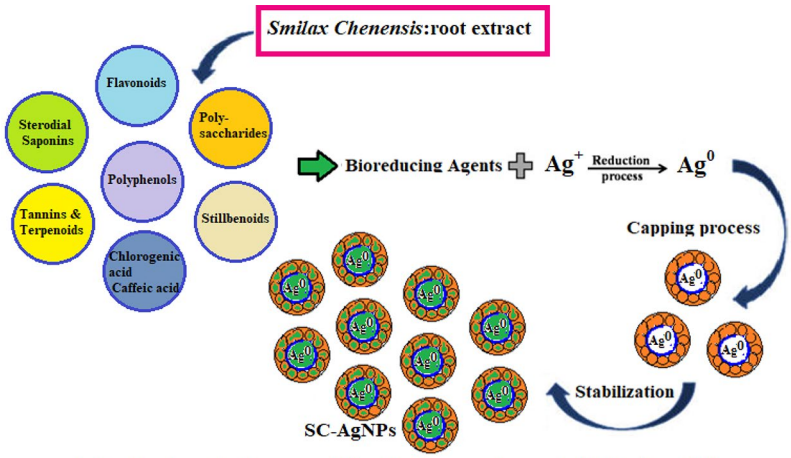

A simple schematic diagram of bioreduction, capping and stabilization of Silver nanoparticle by bioactive compounds of root extract of Smilax Chenensis

708.17 and 579.03 cm^{-1} of root extract and 630.88 cm^{-1} of SC-AgNPs respectively are due to aliphatic iodo compounds of C–I stretch. So in conclusion, it is very clearly evident that the different bioactive components like flavonoids, terpenoids, quinuones, polyphenols and steroids of the root extract might have been actively participated in reduction of silver nitrate to SC-AgNPs and in capping and stabilization of the SC-AgNPs. A simple schematic diagram was shown below for easy understanding of bio-reduction, capping and stabilization of silver nanoparticles (SC-AgNPs).

Similar types of results were reported on FT-IR analysis by other researchers on AgNPs synthesised by different parts of medicinal plants by green methods[17–22,39,40,63,64].

Particle size and zeta potential analysis of SC-AgNPs

The particle size analysis of SC-AgNPs was carried out by DLS method. It's an important method to detect the size of green synthesized nanoparticles in an aqueous colloidal solution. The SC-AgNPs will be always in Brownian movement in the diluted colloidal solution and the scattered light intensity with time calculated. The result reveals that the size of SC-AgNPs were in the range of 12.8–90.2 nm, with an average mean size of 45.6 nm ± 2 nm, with cumulative Z average of 39.5 nm ± 2 nm. The poly disperse index (PDI) of SC-AgNPs is around 0.193 indicating that the particles are poly dispersed in nature (Fig. 3a). The stability of the SC-AgNPs depends upon Zeta potential and it is a physical property which gives the net surface charge of the nanoparticles, in the present study the net surface charge of green synthesized SC-AgNPs was detected to be negatively charge around − 21 mV shown in (Fig. 3b). The results revealed that the SC-AgNPs have high zeta potential value of − 21 mV, which gives rise to more stability in aqueous colloidal solution. Due to these reason the SC-AgNPs in colloidal solution were well dispersed without any agglomeration for prolonged period of time[17–20].

XRD analysis of SC-AgNPs

X-ray diffraction studies of green synthesized SC-AgNPs was done to understand the crystalline nature of the particles. The XRD pattern of green synthesized SC-AgNPs in shown in Fig. 4a, it reveals four distinct reflections in the diffractogram at 38.3° (111), 44.8° (200), and 65.15° (220) and 78.27° (311) respectively. The results are in accordance to JCPDS card data: 03–0931, indicating that the SC-AgNPs were crystalline in nature with face central cubic structure, it is also concluded that there are no additional reflections other than Ag lattice, indicates that the SC-AgNPs are very stable and are not affected by any other external molecules present in the root extract. The average grain size of SC-AgNPs was calculated by Scherrer equation found to be around (38.3°) 17. 57 nm, (44.8°) 22.45, (65.15°) 32.84 nm, (78.27°) 35.67 nm ± 2 nm. The results were similar to DLS. TEM and AFM analysis of green synthesized SC-AgNPs. Similar type of results were observed by green synthesized AgNPs by other plants such as *Drosera spatulata* Labill var. bakoensis(17), *Dovyalis caffra* fruit extract(23) callus extract of *C. camphora*(24), *Panicum milliaceum* grains extract (25), *Allium sativum* flower extract (26) also revealed similar type of results in XRD analysis.

AFM analysis of SC-AgNPs

The 2D image analysis of SC-AgNPs by AFM studies reveals the surface morphology and topology of green synthesized SC-AgNPs, reveals that the nanoparticles were spherical in shape. The size of the green synthesized SC-AgNPs were within the range of 10 nm to 30 nm. The average grain size was around 29.480 ± 1 nm (Fig. 4b (i-iii)). The Sample area 250,000 nm*nm; and the Mean values are as follows, Min 0.000 nm Max: 29.480 nm; Peak to peak 29.480 nm; Root mean square RMS 4.469 nm; the Sa, the Average roughness of the particles is 3.354 nm of the green synthesizd SC-AgNPs. The other important parameters to be consider in grain analysis of SC-AgNPs are as follows: The Sq root mean square height of the surface 4.469 nm; Sa, Arithematical mean height of the surface 3.334 nm Sku Kurtosis of height distribution 3.156; ssk Skewness of height distribution 0.241. Sz Maximum height of the surface 29.480 nm; S10z, Ten points height 27.115 nm; Sp, Maximum peak height 16.347 nm; Sv, Minimum valley depth 13.133 nm. The maximum area of peak height is 16.347 nm and the maximum area of valley depth is 13.133 nm (Fig. 4b (i-iii)). Another important analysis was carried using 3D AFM image of SC-AgNPs to detect the grain or particle size distribution by Z-coloration method using Nova

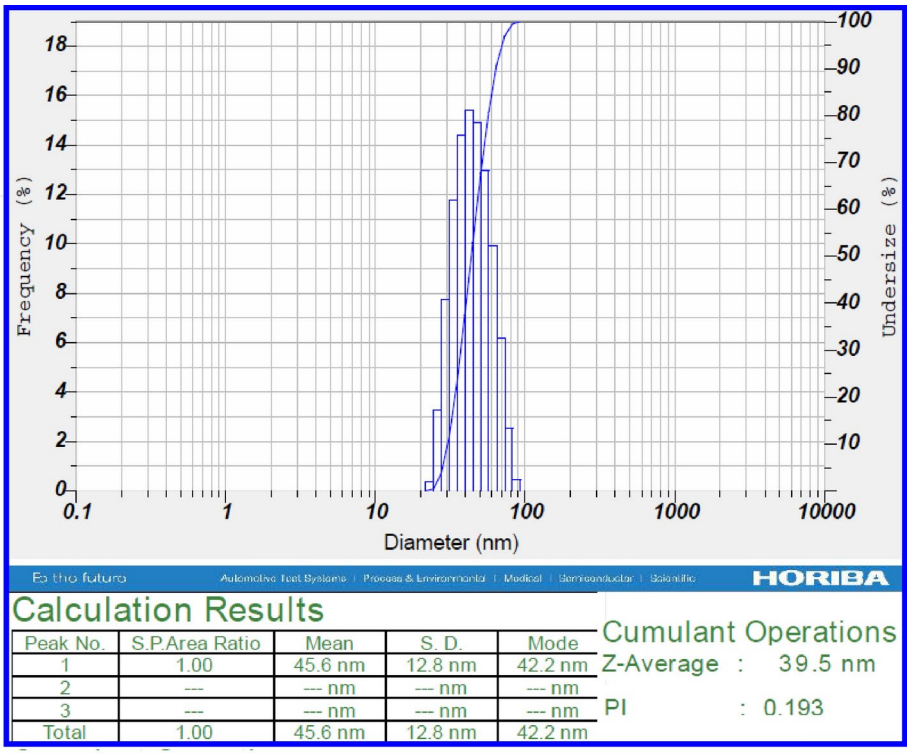

(a)

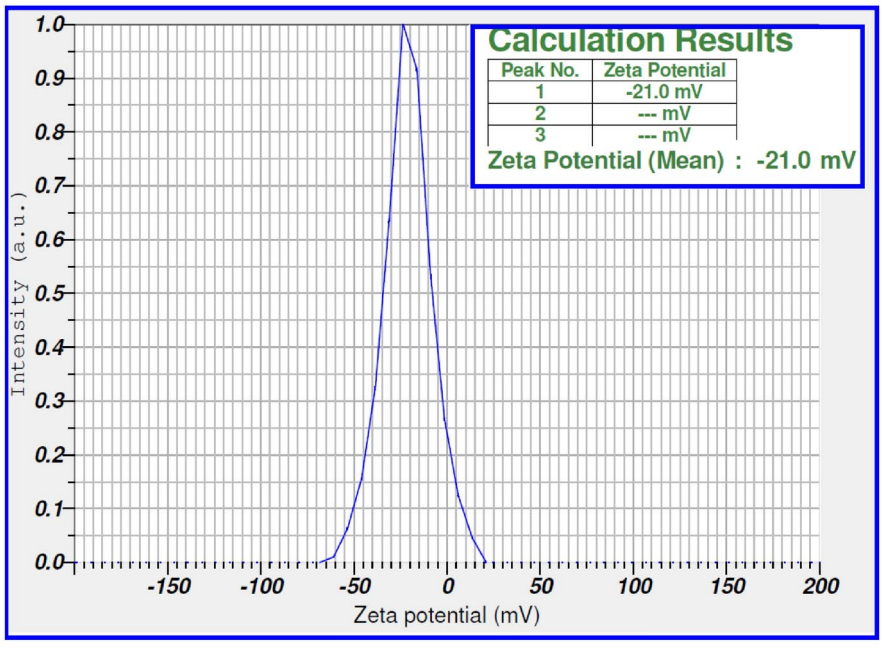

(b)

Fig. 3. (**a**) Particle size analysis of green synthesized SC-AgNPs. (**b**) Zeta potential analysis of green synthesized SC-AgNPs.

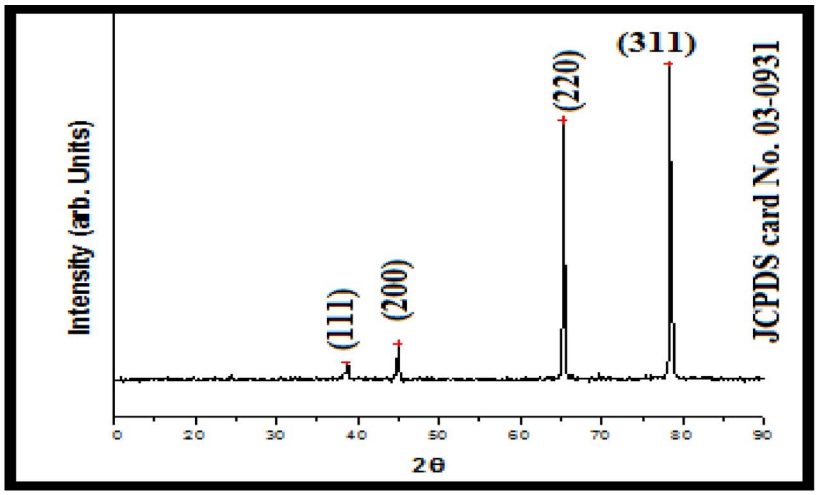

(a)

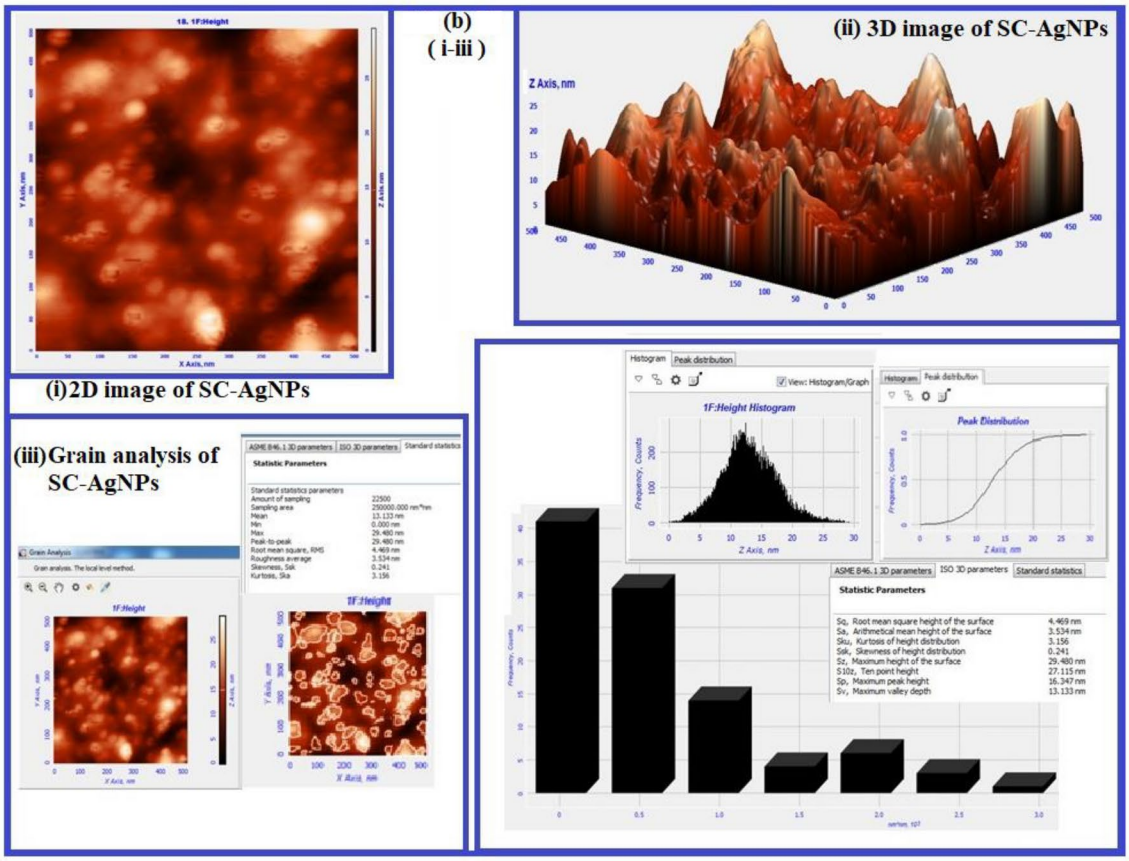

Fig. 4. (**a**) XRD analysis of SC-AgNPs. (**b**) [i] 2D image of SC-AgNPs [ii] 3D image of SC-AgNPs [iii] Grain analysis of SC-AgNPs to detect particle size and shape and surface morphology and topology by AFM. [iv] 3D image of SC-AgNPs to detect Particle size distribution by Z-coloration analysis by AFM Nova-pixel software. (**c**–**g**) TEM analysis of SC-AgNPs: (**c**,**d**) TEM images at 50 nm scale bar, (**e**) SAED pattern of SC-AgNPs, (**f**,**g**) Size distribution calculation of SC-AgNPs by J image histograms.

pixel software provide by the vender along with AFM instrument. The particle size distribution in 3D image reveals that the particles are in the range of 5 nm to 29 ± 1 nm (Fig. 4b (iv)). Further, TEM studies also revealed that the green synthesized SC-AgNPs were mostly spherical in shape Similar type of results were also reported by green synthesized silver nanoparticles by an insectivorous plant[17].

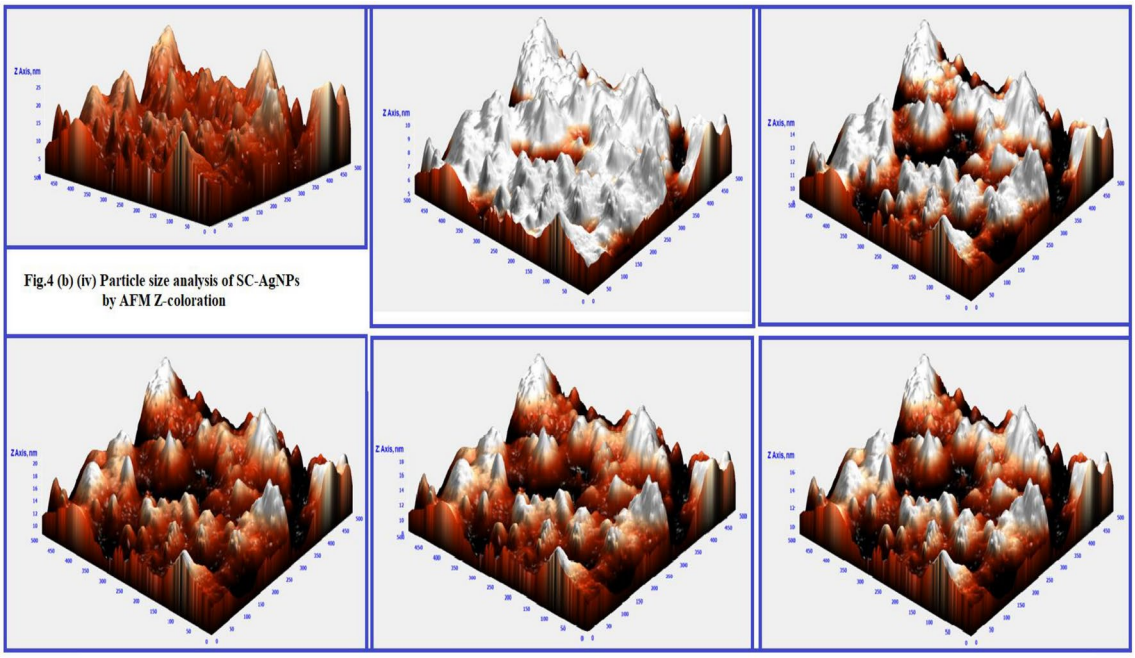

Fig.4 (b) (iv) Particle size analysis of SC-AgNPs by AFM Z-coloration

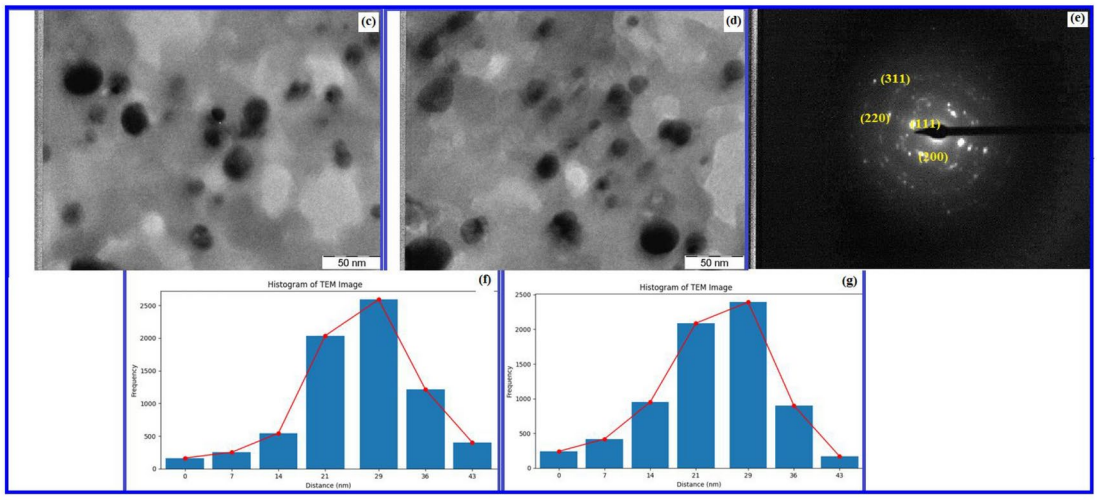

Figure 4. (continued)

TEM analysis of SC-AgNPs

The Transmission electron microscopy studies of green synthesized SC-AgNPs was used to detect the exact size and shape of the nanoparticles. The results revealed that the size of SC-AgNPs were in the range of 10 nm ± 2 nm to 45 nm ± 2 nm with spherical in shape with an average size of 35 nm ± 5 nm (Fig. 4c–g). Interestingly the results were similar to our DLS data and AFM data reported by previous researchers on green synthesized metal nanoparticles[17–22]. The SAED pattern data also reveals the planes of diffractions similar to 2θ data of XRD analysis which is as follows 111, 200, 220, 311 which corresponds 38.3° (111), 44.8° (200), and 65.15° (220) and 78.27° (311) respectively. Similarly the green synthesized AgNPs by other plants such as *Drosera spatulata* Labill var. Bakoensis (17), *Dovyalis caffra* fruit extract(23) callus extract of *C. camphora(24)*, *Clarias gariepinus(13) Lawsonia inermis(14), Bakers Yeast(16) and Trichoderma saturnisporum(15)*also revealed similar type of results in TEM and SAED pattern.

Bactericidal activity of SC-AgNPs

The bactericidal activity of green synthesized SC-AgNPs was used to find out the efficacy of the nanoparticles on both gram -ve and gram + ve bacterial strains. The results revealed that the SC-AgNPs have very good antibacterial activity against both bacterial species viz., gram –ve *Escherichia coli* and *Pseudomonas aeruginosa and* gram + ve *Staphylococcus aureus* and *Bacillus megatrium*. The zone of inhibition (ZOI) at different concentrations of 10 mcg, 20 mcg, 30 mcg of SC-AgNPs along with standard antibiotic (Amoxycillin 10 mcg, Biogram AMX10) and root extract of *Smilax china* L were shown in Fig. 5a, the ZOI were measured in mm and the values were

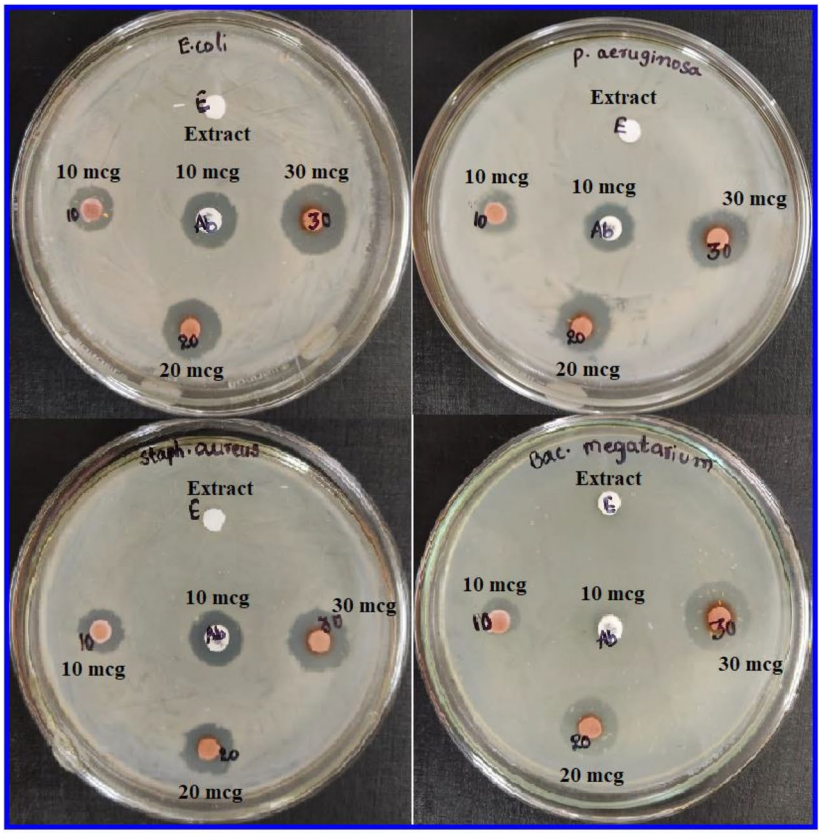

(a)

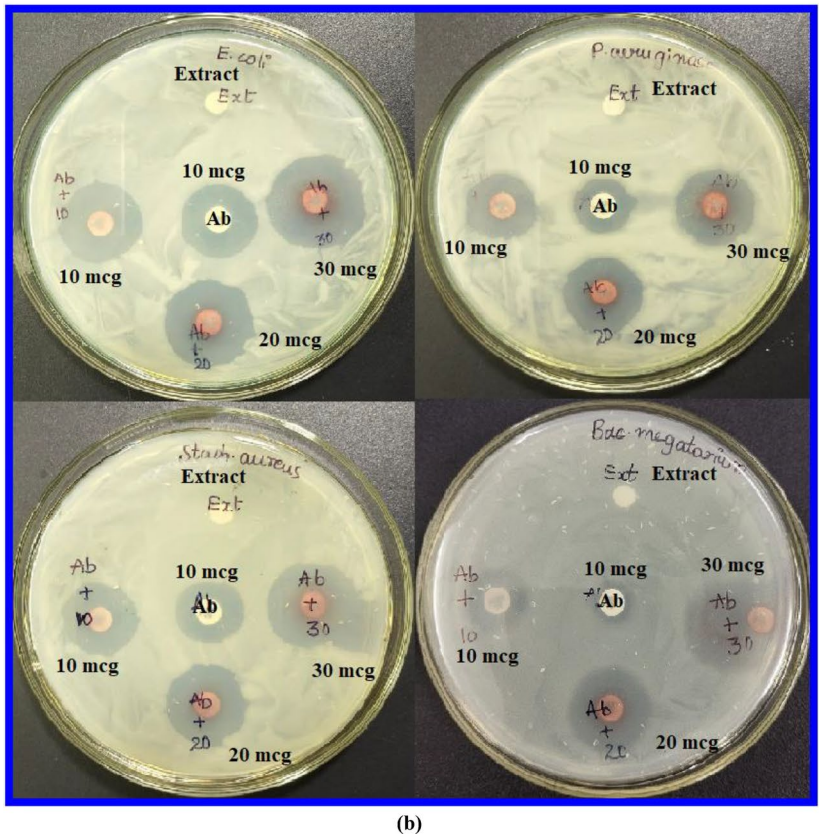

(b)

Fig. 5. (**a**) Antimicrobial Activity of SC-AgNPs. (**b**) Antimicrobial Activity of SC-AgNPs coupled with Antibiotic (10 mcg of Amoxycillin). (**c**) Graphical representation of Antimicrobial Activity of SC-AgNPs& SC-AgNPs coupled with Antibiotic (10 mcg of Amoxycillin). (**d**) Schematic diagram of Antibacterial activity of Green synthesized SC-AgNPs and SC-AgNPs coupled with Antibiotic.

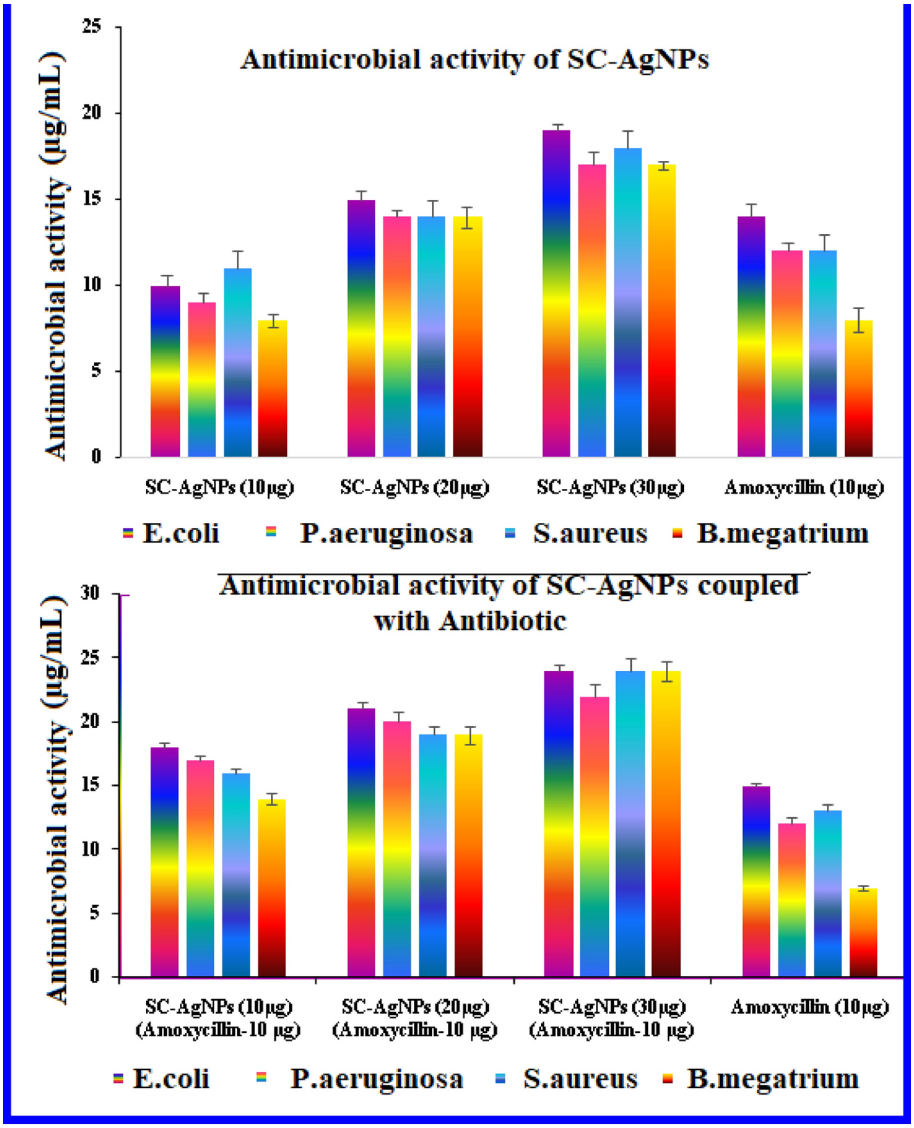

(c)

Figure 5. (continued)

tabulated in Table 1. The above results revealed that the SC-AgNPs have efficient antibacterial activity on the both gram -ve and gram + ve bacterial strains, the bactericidal activity was concentration dependent, higher the concentration higher the ZOI. Fascinatingly, the green synthesized SC-AgNPs reveals good antibacterial activity even at lower concentrations when compared with standard antibiotic, and at the higher concentrations (30 mcg) of SC-AgNPs showed outstanding antibacterial activity then the standard antibiotic. The results are as follows: The zone of inhibition against gram -ve *Escherichia coli* is as follows: 10 mm (10 mcg), 15 mm (20 mcg) and 19 (30 mcg) for SC-AgNPs and Antibiotic 14 mm (10 mcg), and SC-root extract 00 mm (30 mcg), and ZOI for *Pseudomonas aeruginosa* 09 mm (10 mcg), 14 mm (20 mcg) and 17 (30 mcg) for SC-AgNPs and Antibiotic 12 mm (10 mcg), and SC-root extract 00 mm (30 mcg). and gram + ve *Staphylococcus aureus* is as follows: 11 mm (10 mcg), 14 mm (20 mcg) and 18 (30 mcg) for SC-AgNPs and Antibiotic 12 mm (10 mcg), and SC-root extract 00 mm (30 mcg),and *Bacillus megatrium,* is as follows: 08 mm (10 mcg), 14 mm (20 mcg) and 17 (30 mcg) for SC-AgNPs and Antibiotic 08 mm (10 mcg), and SC-root extract 00 mm (30 mcg) Similar results by other nanoparticles were also reported by different scientist working in the area of nano-materials Similar type of results with the whole plant extract of *Drosera spatulata* Labill var. bakoensis(17) and leaf extract of *Argyreia nervosa*[19] and *Decaschistia crotonifolia*[20], flower extract of *Aerva lanata*[21] leaf extract of *Britneria herbeae*[63], & bark extract of *S mahagoni*[64] revealed very good antibacterial activity on both gram –ve and gram + ve. At th same time the AgNPs synthesized by other plant extract like *Dovyalis caffra* fruit extract (23) callus extract of *C. camphora(24)*, *Panicum milliaceum* grains extract (25), *Allium sativum* flower extract (26) also revealed good to excellent antibacterial activity on different pathogenic bacteria.The graphical representations of bacterial activity were drawn using MS-office Excel software.

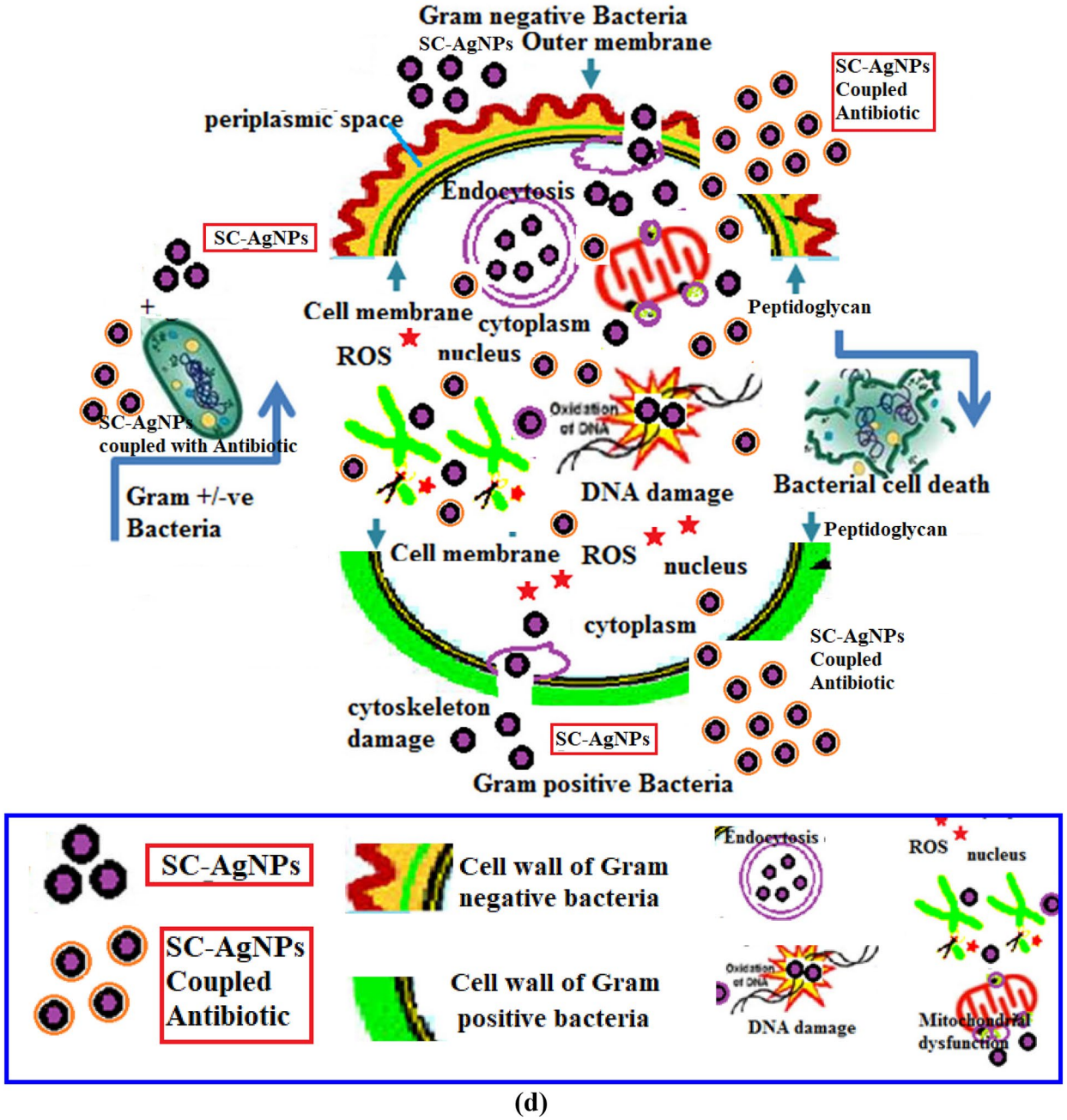

(d)

Figure 5. (continued)

Bactericidal activity of SC-AgNPs coupled with antibiotic

So, in the present study, the SC-AgNPs coupled with antibiotic (Amoxycillin 10 mcg, Biogram AMX10) revealed an outstanding antibacterial activity, when compared with SC-AgNPs and antibiotic alone. Indicating that the metal nanoparticles coupled antibiotics with a small dosage can be effective and efficient antimicrobial agents. The ZOI of antibiotic, SC-AgNPs coupled antibiotic were shown in Fig. 5b, they were measured in mm and the results were tabulated in Table.1. The zone of inhibition against gram -ve *Escherichia coli* is as follows: 18 mm (10 mcg), 21 mm (20 mcg) and 24 (30 mcg) for SC-AgNPs coupled with 10 mcg of Amoxycillin and Antibiotic 15 mm (10 mcg), and SC-root extract 00 mm (30 mcg), and ZOI for *Pseudomonas aeruginosa* 17 mm (10 mcg), 20 mm (20 mcg) and 22 (30 mcg) for SC-AgNPs coupled with 10 mcg of Amoxycillin and Antibiotic 12 mm (10 mcg), and SC-root extract 00 mm (30 mcg). *and* gram + ve *Staphylococcus aureus* is as follows: 16 mm (10 mcg), 19 mm (20 mcg) and 24 (30 mcg) for SC-AgNPs coupled with 10 mcg of Amoxycillin and Antibiotic 13 mm (10 mcg), and SC-root extract 00 mm (30 mcg),and *Bacillus megatrium,* is as follows: 14 mm (10 mcg), 19 mm (20 mcg) and 24 (30 mcg) for SC-AgNPs coupled with 10 mcg of Amoxycillin and Antibiotic 07 mm (10 mcg), and SC-root extract 00 mm (30 mcg). These days, antibacterial resistance is a most important problem in the neighbourhood, due to use of antibiotics prolonged period which lead to antibacterial resistance.

	Smilax china root extract	Antibiotic (Amoxycillin-10 mcg)	SC-AgNPs (10 mcg)	SC-AgNPs (20 mcg)	SC-AgNPs (30 mcg)
Zone of Inhibition (mm)					
E.coli	00	14 mm	10 mm	15 mm	19 mm
P.aeruginosa	00	12 mm	09 mm	14 mm	17 mm
S.aureus	00	12 mm	11 mm	14 mm	18 mm
B.magatarium	00	08 mm	08 mm	14 mm	17 mm
	***Smilax china* root extract**	**Antibiotic (Amoxycillin-10 mcg)**	**Amoxycillin-10 mcg + SC-AgNPs (10 mcg)**	**Amoxycillin-10 mcg + SC-AgNPs (20 mcg)**	**Amoxycillin-10 mcg + SC-AgNPs (30 mcg)**
Zone of Inhibition (mm)					
E.coli	00	13 ± 1 mm	18 mm	21 mm	24 mm
P.aeruginosa	00	12 mm	17 mm	20 mm	22 mm
S.aureus	00	12 ± 1 mm	16 mm	19 mm	24 mm
B.magatarium	00	07 ± 1 mm	14 mm	19 mm	24 mm

Table 1. (i): Antimicrobial activity of SC-AgNPs. (ii): Antimicrobial activity of SC-AgNPs Coupled with 10 mcg a moxycillin.

Presently, scientists and researchers have been widely working on antimicrobial activity by using different metal nanoparticles. The outcome of their work revealed promising results, that the different metal nanoparticles exhibits superior to outstanding antimicrobial activity when compared with standard antibiotics which was useful to overcome the antimicrobial resistance and also to overcome the present problem. The earlier studies on metal nanoparticles reveal that the shape and size of silver nanoparticles plays an important role in the antimicrobial processes and cause lethal effect when they come in contact with the bacterial surface. These metal nanoparticles attach to the cell surface and disturb the cell wall of the bacteria and penetrate the bacterial cell and cause interruption in permeability and respiration of bacteria and also induce DNA damage and elevate ROS stress and which lead to interruption of ATP production, causing uncontrollable ion transport through cell membrane and finally cause bacterial cell death. So in conclusion, the SC-AgNPs have excellent antimicrobial activity due their small size and spherical shape[17–20,41–44,63,64]. The green synthesized silver nanoparticles reveals superior antibacterial activity[65], and at the same time the silver nanoparticles combined with antibiotic also reveals efficient activity against antibiotic-resistant bacteria[66] shown in [Fig. 5c], an another study by aqueous callus extract of *Fagonia indica* also revealed excellent activity[67]. Another study confirmed that, the silver nanoparticles combined with antibiotics revealed excellent synergistic effect against gram-positive and gram-negative bacteria[68]. Another important study also reported that silver nanoparticles combined with antibiotics show high impact on the cell membrane, causing enhanced damage thus lead to the death of bacterial cells rapidly and efficiently[69]. An important study by biosynthesized silver nanoparticle based antibiotic conjugates also revealed improved antibacterial activity[70,71]. At the same time synergism of silver nanoparticles along with antibiotics can be adopted as the best Alternative Treatment for Multi-resistant bacterial pathogens[72–76]. The antibacterial activity of both SC-AgNPs and SC-AgNPs coupled with antibiotic was shown in Fig. 5d as a schematic diagram below.

Antioxidant activity of SC-AgNPs by DPPH assay

Since, several decades' scientists have been continuously working to find out suitable antioxidants by using various plant sources and their bioactive compounds as natural antioxidants to protect the human population from several human disorders which are caused by oxidative stress. It is well known that the cells consists of unstable molecules such as oxygen, this oxygen molecules readily react with other molecules in the cellular system and form reactive oxygen species (ROS), which is dangerous sign in the living system which very harmful to the body. These ROS molecules readily and easily react with DNA, RNA, proteins and lipids of the cell and cause cell death and they also cause oxidative stress in various human cells and cause disorders like inflammation, cancer and ageing and other neurodegenerative disorders. So it is very vital and practical to find out suitable antioxidants which can reduce ROS. So, depending on the necessity and significance of antioxidants several researchers have been working on plant bioactive components, and they also started working on metal nanoparticles which are synthesized by plant sources exhibit superior antioxidant activity as an alternative sources of antioxidants. In the present study, in vitro antioxidant activity of the SC-AgNPs was determined by different free radical scavenging assays. The antioxidant activity of green synthesized SC-AgNPs along with root extract of *Smilax china* L. (SC-RE) and standard Ascorbic acid was carried out by DPPH scavenging assay. The results revealed that the (SC-RE) showed moderate antioxidant activity, where as SC-AgNPs revealed excellent antioxidant activity on par with standard Ascorbic acid. The Sc-AgNPs revealed concentration dependent scavenging activity, higher the concentration more the scavenging activity, the results are shown in Fig. 6a the values were tabulated in Table 2. (i). *Smilax china* L. root extract (SC-RE) and SC-AgNPs showed the maximum inhibition of 62.68% and 76.22% and standard Ascorbic acid inhibition 72.28% respectively against DPPH free radicals at the highest concentration of 100 µg/mL used in this assay. The DPPH activity of SC-AgNPs (76.22%) is greater than the standard ascorbic acid (72.28%) at the highest concentration. So, it is concluded that the green synthesized SC-AgNPs have superior antioxidant activity. There are several earlier reports, which reveal similar

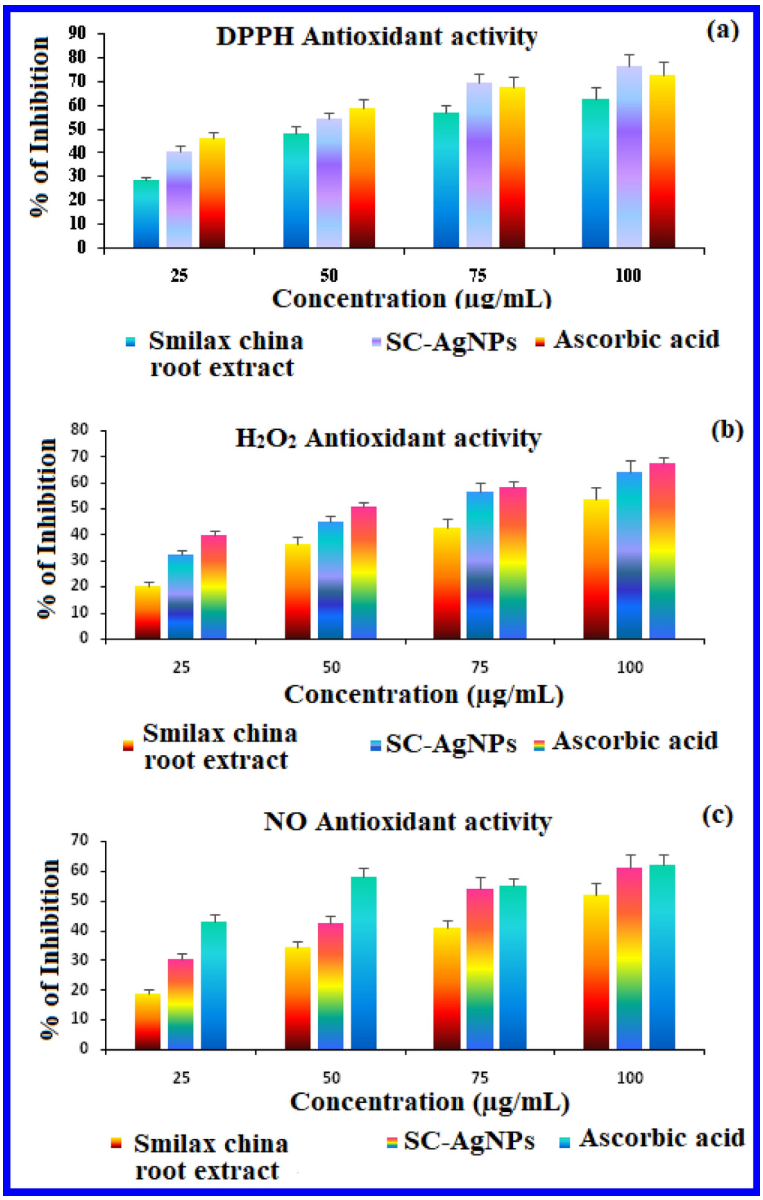

Fig. 6. (**a**–**c**) Antioxidant activity of SC-AgNPs. (**d**) Schematic diagram of free radical scavenging activity of plant extract and green synthesized SC-AgNPs.

type of results with silver nanoparticles[17–22,41–44,63,64]. Not only SC-AgNPs other silver nanoparticles fabricated by plant sources can be useful as future antioxidant agents.

Antioxidant activity of SC-AgNPs by H_2O_2

The in vitro antioxidant activity of the green synthesized SC-AgNPs, root extract of *Smilax china* L. (SC-RE) and standard Ascorbic acid was also determined by H_2O_2 free radical scavenging assay. The results illustrate that the (SC-RE) showed minimum to moderate antioxidant activity, where as SC-AgNPs revealed good antioxidant activity when compared with standard Ascorbic acid. The antioxidant activity of SC-AgNPs revealed that it is concentration dependent. The scavenging activity results were shown in Fig. 6b the values were tabulated in Table 2 (ii). *Smilax china* L. root extract (SC-RE) and SC-AgNPs showed the maximum inhibition of 53.64% and 64.26% and standard ascorbic acid inhibition 67.28% respectively against H_2O_2 free radicals scavenging activity at the highest concentration of 100 µg/mL used in this assay.

Antioxidant activity of SC-AgNPs by NO

In vitro antioxidant activity of the green synthesized SC-AgNPs along with root extract of *Smilax china* L. (SC-RE) and standard Ascorbic acid was also determined Nitric Oxide free radical scavenging assay. The results revealed that the (SC-RE) showed moderate antioxidant activity, where as SC-AgNPs revealed very good antioxidant activity when compard with standard Ascorbic acid. Here also the Sc-AgNPs revealed concentration dependent

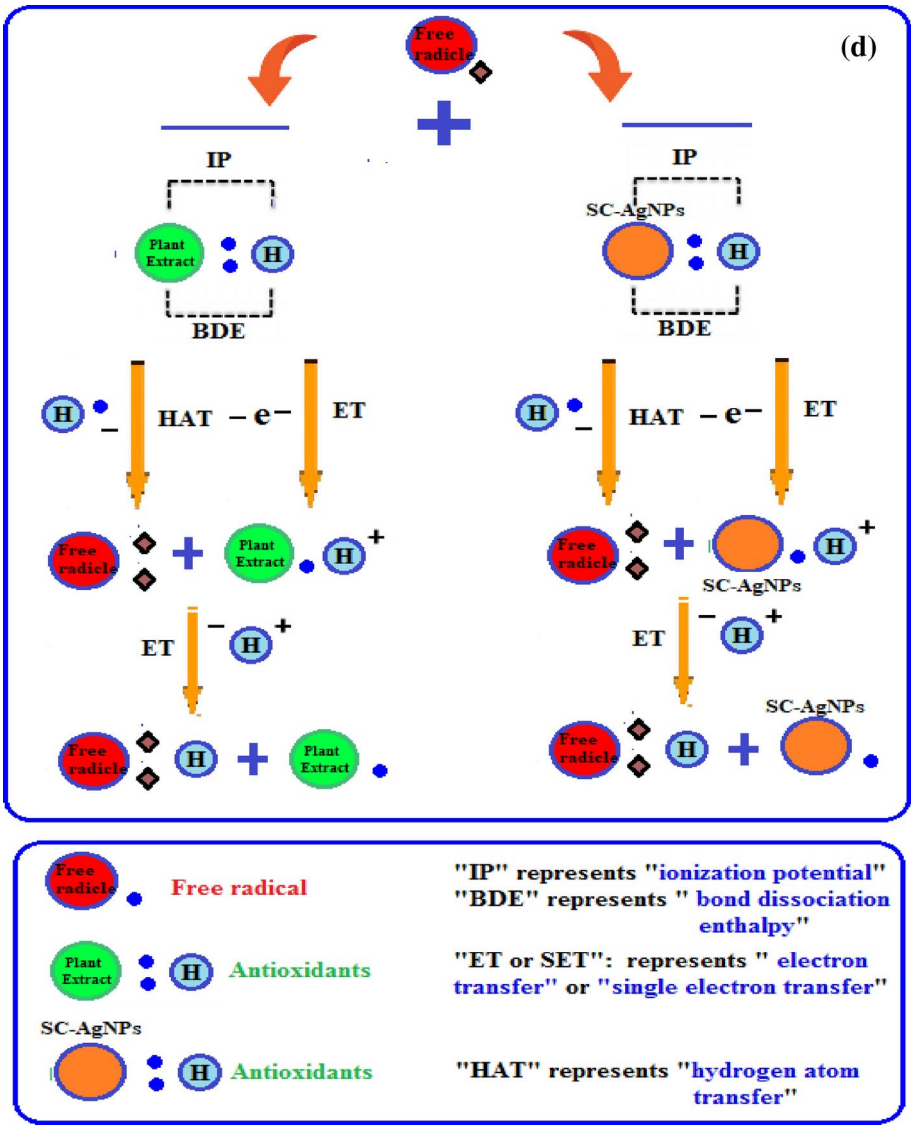

Figure 6. (continued)

(i)DPPH method	Free radical scavenging activity ± SD (%)			
Sample name	**25 µg/mL**	**50 µg/mL**	**75 µg/mL**	**100 µg/mL**
Smilax china root extract	28.27 ± 0.83	48.24 ± 0.48	56.64 ± 0.42	62.68 ± 0.32
SC-AgNPs	40.42 ± 0.36	54.08 ± 0.92	69.26 ± 0.54	76.22 ± 0.74
Ascorbic acid	46.04 ± 0.22	58.64 ± 0.26	67.44 ± 0.56	72.28 ± 0.62
(ii)H_2O_2 method	**Free radical scavenging activity ± SD (%)**			
Sample name	**25 µg/mL**	**50 µg/mL**	**75 µg/mL**	**100 µg/mL**
Smilax china root extract	20.34 ± 0.62	36.60 ± 0.12	42.64 ± 0.26	53.64 ± 0.32
SC-AgNPs	32.24 ± 0.72	44.82 ± 0.28	56.42 ± 0.48	64.26 ± 0.58
(iii)NO method	**Free radical scavenging activity ± SD (%)**			
Sample name	**25 µg/mL**	**50 µg/mL**	**75 µg/mL**	**100 µg/mL**
Smilax china root extract	18.64 ± 0.46	34.30 ± 0.84	40.82 ± 0.88	52.28 ± 0.42
SC-AgNPs	30.42 ± 0.68	42.48 ± 0.28	54.26 ± 0.48	60.98 ± 0.28

Table 2. (i): Free Radical Scavenging activity of SC-AgNPs by DPPH method. (ii) Antioxidant activity of SC-AgNPs by H_2O_2 method. (iii) Antioxidant activity of SC-AgNPs by Nitric oxide (NO) method.

free radical scavenging activity, higher the concentration more the scavenging activity. The results are shown in Fig. 6c the values were tabulated in Table 2 (iii). *Smilax china* L. root extract (SC-RE) and SC-AgNPs showed the maximum inhibition of 52.28% and 60.98% and standard Ascorbic acid inhibition 62.20% respectively against DPPH free radicals at the highest concentration of 100 µg/mL used in this assay. At the same time the graphical representation of antioxinadt activity were drawn using MS-office Excel software. The DPPH activity of SC-AgNPs (60.98%) is almost equivalent to the standard ascorbic acid (62.20%) at the highest concentration. In conclusion the results revealed that the DPPH activity is best method among the three methods, which reveals highest free radical scavenging activity then standard Ascorbic acid, followed by H_2O_2 and NO methods. The antioxidant activity of plant extract and silver nanoparticles is represented in a schematic diagram below in Fig. 6d.

Cytotoxic activity of SC-AgNPs on MDA-MB-231 (human breast *cancer* cell line)

MTT assay was carried out to find out the cytotoxic effect of green synthesized SC-AgNPs and cell viability of MDA-MB-231 (Human breast cancer cell line) treated with different concentrations of SC-AgNPs. In the present study the MDA-MB-231 (human breast cancer cell line) cells were treated with different concentrations SC-AgNPs 10 µg/mL, 25 µg/mL; 50 µg/mL; 100 µg/mL and Control (without nanoparticles treatment) for 24 h (Fig. 7a). After 24 h the IC_{50} values were calculated. The IC_{50} value was determined by using linear regression equation i.e. $Y = Mx + C$. Here, $Y = 50$, M and C values were derived from the viability graph (Fig. 7b).

$$\%\ \text{Cell Viability} = \frac{\text{Mean Absorbance of Sample} - \text{Blank}}{\text{Mean absorbance of Untreated} - \text{Blank}} * 100$$

The IC_{50} value of SC-AgNPs was calculated by statistical data of cell cytotoxicity studies reveals that IC_{50} value of 33.98 µg/mL. It is concluded that cytotoxicity of SC-AgNPs is dosage dependent manner from lower concentration to higher concentration as the concentration increase the cell viability decreases shown in Fig. 7b. From these results it revealed that SC-AgNPs have excellent anticancer nature, and revealed superior cytotoxic potency against MDA-MB-231 cancer cells. Similar type of results were also reported by other green synthesized silver nanoparticles, such as the biosynthesized silver nanoparticles using extract of *nepeta deflersiana* against human cervical cancer cells (HeLA) revealed excellent cytotoxic activity[76], and *Seripheidium quettense* aqueous extract mediated biogenic silver nanoparticles revealed several important theranostic applications viz anticancer activity[77]. Another study using Asian spider flower reveals best in vitro cytotoxic activity against human breast carcinoma cells[78]. *Mentha arvensis* (Linn.)-plant mediated silver nanoparticles reveals concentration dependent cell death in MCF7 and MDA-MB-231 cancer cells, and Silver–palm pollen nanocomposite also exhibits antiproliferative and proapoptotic properties on MCF-7 breast cancer cells[79,80]. *Mentha longifolia* plant extract mediated silver nanoparticles also reveals therapeutic potential against HCT116 colon cancer[81]. Similarly the green synthesized SC-AgNPs also showed excellent cytotoxic and anti-proliferative activity with very minimal concentration of Sc-AgNPs. From the above results it is concluded that in future the SC-AgNPs can be adopted as anticancer agent. At the same time it's very essential to establish and detect the molecular mechanism behind anticancer properties of the SC-AgNPs which will carried out in future studies (Table 3).

Photo-catalytic reduction of cotton blue dye degradation by SC-AgNPs

At present, the world is rapidly marching towards rapid industrialization, which can lead to high contamination of soil, air and water bodies. Thus the effluents discharged from textile industries contaminates the ground water and also drinking water resources which leads to several kinds of toxic effects on gastrointestinal tract problems, skin and eye irritation problems[82–84]. At present an important study was carried out to detect the photo-catalytic reduction of cotton blue (CB) dye for specific time interval was carried out by using green synthesized SC-AgNPs by the detoxification method. The catalytic degradation of CB dye was analyzed in the presence of the green synthesized SC-AgNPs was determined by their color change. The color intensity of CB dye was reduced from dark blue to light blue as the time increases from 0 to 30 min, thus confirming the successful catalytic dye degradation activity of the green synthesized SC-AgNPs. The results of the absorbance OD values were recorded and the results were shown in (Fig. 8a, b). The results reveal the OD values of CB dye at 0 min is 1.861, and after addition of SC-AgNPs at 0 min-1.526, 5 min-1.167, 10 min-0.969, 15 min-0.720 and 20 min-0.331, 25 min-0.243 and 30 min-0.135. In conclusion the green synthesized SC-AgNPs can be used as effective catalytic agents against dye degradation, so it is proven that silver nanoparticles enhances phyto-catalytic dye degradation. It is well known that the CB dye is wildly used in textile industry, in this experiment CB dye was exposed for a known time interval of 0–30 min by the addition of SC-AgNPs, showed a significant decrease in the peak and color intensity [Fig. 8(a, b)]. Hence, confirming degradation of dye was due to the SPR property of the green synthesized SC-AgNP. Similar type of results was reported by FF-AgNPs and PVP coated FF-AgNPs[85], similar results were also observed in the case of the Crystal violate dye degradation study by using Cd-AgNPs[86].

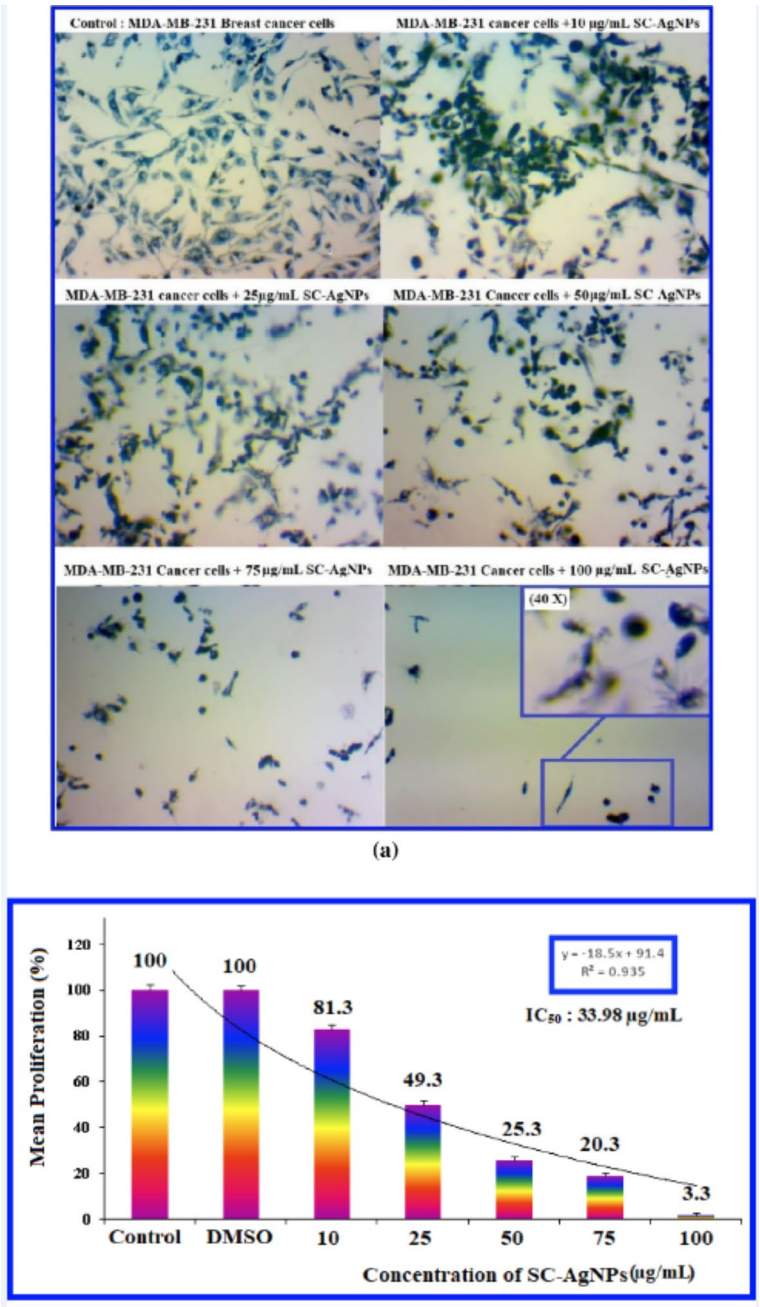

Fig. 7. (**a**) Anticancer activity of SC-AgNPs in MDA-MB-231 (human breast cancer cell lines). (**b**) Antiproliferative activity of SC-AgNPs in MDA-MB-231 (human breast cancer cell lines) Calculation of IC_{50} Value: 33.98 µg/mL.

Conclusion

In current study we hereby report a prompt and proficient method for green synthesis of silver nanoparticles using root extract of *Smilax chineses* or *Smilax china* L. commonly known has 'Chinese root' or 'China root'. The green synthesized SC-AgNPs were analyzed by various advanced diverse spectroscopic methods viz., the UV visible SPR spectra of SC-AgNPs was obtained at 432 nm and FT-IR spectra of SC-AgNPs confirmed that different bioactive molecules of root extract were actively involved in reduction and stabilization of SC-AgNPs. Further, the particle size of SC-AgNPs was detected to be poly-dispersed in nature within the range of 12.8 nm to 90.2 nm, with an average mean size of 45.6 nm ± 2 nm, with cumulative Z average of SC-AgNPs is 39.5 nm ± 2 nm and the poly disperse index (PDI) of SC-AgNPs was detected to be around 0.193 and the zeta-potential was determined to be around at −21 mV, which indicates the stability of SC-AgNPs the colloidal aqueous solution. Additional the nanoparticles were analyzed by TEM and AFM, indicating that SC-AgNPs were spherical in shape. Further more extensive studies were carried out to detect the therapeutic applications of SC-AgNPs. The results revealed that SC-AgNPs have excellent antimicrobial activity, antioxidant activity, anticancer activity and

Conc.in µg/mL	Proliferation percentage
Control	100
DMSO	100
SC-AgNPs-10 µg/mL	81.3
SC-AgNPs-25 µg/mL	49.3
SC-AgNPs-50 µg/mL	25.3
SC-AgNPs-75 µg/mL	20.3
SC-AgNPs-100 µg/mL	3.3

Table 3. Cytotoxic activity of SC-AgNPs on MDA-MB-231 cells (Human breast cancer cell line).

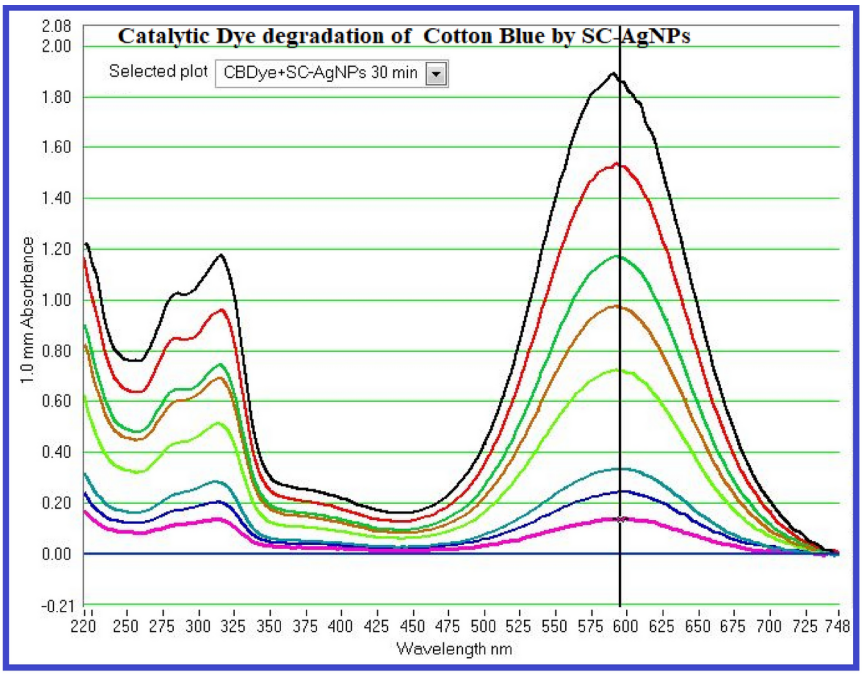

Fig. 8. (**a**) Photo-catalytic activity of SC-AgNPs on Cotton blue dye degradation. (**b**) Photo-catalytic dye degradation by SC-AgNPs.

efficient industrial photo-catalytic activity. The SC-AgNPs coupled with antibiotic were proved to have excellent antibacterial activity against gram + ve and gram –ve bacteria and can be useful as future antimicrobial agents to overcome a major current problem antibacterial resistance. The SC-AgNPs reveals superior antioxidant activity by DPPH method when compared with other two methods. They also revealed excellent cytotoxic and anti proliferative effect on MDA-MB-231 (Human breast cancer cell line) in dose dependent manner, with an IC_{50} value of 33.98 µg/mL. It is well known that environmental pollution due rapid industrialization is a major problem. The SC-AgNPs were proved to be very good industrial dye degradation agents. Hence, in conclusion the green synthesized SC-AgNPs revealed multifunctional properties of therapeutic and industrial applications shown in schematic diagram below.

Data availability

All data generated or analysed during this study are included in this submitted article.

Received: 9 June 2024; Accepted: 18 October 2024
Published online: 02 December 2024

References

1. Yaqoob, A. A. et al. Recent advances in metal decorated nanomaterials and their various biological applications: A review. *Front. Chem.* **8**, 341 (2020).
2. Habibullah, G., Viktorova, J. & Ruml, T. Current strategies for noble metal nanoparticle synthesis. *Nanoscale Res. Lett.* **16**, 47 (2021).
3. Salem, S. S., Hammad, E. N., Mohamed, A. A. & El-Dougdoug, W. A comprehensive review of nanomaterials: Types, synthesis, characterization, and applications. *Biointerface Res. Appl. Chem.* **13**, 1–41 (2023).
4. Salem, S. S. & Fouda, A. Green synthesis of metallic nanoparticles and their prospective biotechnological applications: an overview. *Biol. Trace Elem. Res.* **199**, 344–370 (2021).
5. Salem, S. & Salem, A. A mini review on green nanotechnology and its development in biological effects. *Arch. Microbiol.* **205**, 128 (2023).
6. Katas, H. et al. Biosynthesis and potential applications of silver and gold nanoparticles and their chitosan-based nanocomposites in nanomedicine. *J. Nanotechnol.* **2018**, 4290705 (2018).
7. Abid, N. et al. Synthesis of nanomaterials using various top-down and bottom-up approaches, influencing factors, advantages, and disadvantages: A review. *Adv. Colloid Interface Sci.* **300**, 102597 (2022).
8. Kaliammal, R. et al. *Zephyranthes candida* flower extract mediated green synthesis of silver nanoparticles for biological applications. *Adv. Powder Technol.* **32**(11), 4408–4419 (2021).
9. Velsankar, K., Sudhahar, S., Parvathy, G. & Kaliammal, R. Effect of cytotoxicity and antibacterial activity of biosynthesis of ZnO hexagonal shaped nanoparticles by *Echinochloa frumentacea* grains extract as a reducing agent. *Mater. Chem. Phys.* **239**, 121976 (2020).
10. Velsankar, K., Sudhahar, S., Maheshwaran, G. & Krishna, K. M. Effect of biosynthesis of ZnO nanoparticles via cucurbita seed extract on *Culex tritaeniorhynchus* mosquito larvae with its biological applications. *J. Photochem. Photobiol. B Biol.* **200**, 111650 (2019).
11. Khandel, P., Yadaw, R. K., Soni, D. K., Kanwar, L. & Shahi, S. K. Biogenesis of metal nanoparticles and their pharmacological applications: present status and application prospects. *J. Nanostruct. Chem.* **8**, 217–254 (2018).
12. Nadaf, S. J. et al. Green synthesis of gold and silver nanoparticles: Updates on research, patents, and future prospects. *OpenNano* **8**, 100076 (2022).
13. Alabssawy, A. N. et al. Hindering the biofilm of microbial pathogens and cancer cell lines development using silver nanoparticles synthesized by epidermal mucus proteins from *Clarias gariepinus*. *BMC Biotechnol.* **24**, 28 (2024).
14. Said, A., Abu-Elghait, M., Atta, H. M. & Salem, S. S. Antibacterial activity of green synthesized silver nanoparticles using *Lawsonia inermis* against common pathogens from urinary tract infection. *Appl. Biochem. Biotechnol.* **196**, 85–98 (2024).
15. Soliman, M. K. Y., Salem, S. S., Abu-Elghait, M. & Salah Azab, M. Biosynthesis of silver and gold nanoparticles and their efficacy towards antibacterial, antibiofilm, cytotoxicity, and antioxidant activities. *Appl. Biochem. Biotechnol.* **195**, 1158–1183 (2023).
16. Salem, S. S. Beaker's yeast–mediated silver nanoparticles. *BioNanoScience* **12**, 1220–1229 (2022).
17. Gaddam, S. A. et al. Multifaceted phytogenic silver nanoparticles by an insectivorous plant *Drosera spatulata* Labill var. bakoensis and its potential therapeutic applications. *Sci. Rep.* **11**, 21969 (2021).
18. Kotakadi, V. S. et al. Bio-inspired multifunctional zinc oxide nanoparticles by leaf extract of *Andrographis serpilifolia* and their enhanced antioxidant, antimicrobial, and antidiabetic activity—a 3-in-1 system. *Part. Sci. Technol.* **40**, 4 (2021).
19. Subramanyam, G. K. et al. *Argyreia nervosa* (Samudra pala) leaf extract mediated silver nanoparticles and evaluation of their antioxidant, antibacterial activity, in vitro anticancer and apoptotic studies in KB oral cancer cell lines. *Artif. Cells Nanomed. Biotechnol.* **49**(1), 635–650 (2021).
20. Palithya, S., Gaddam, S. A., Kotakadi, V. S., Penchalaneni, J. & Challagundla, V. N. Biosynthesis of silver nanoparticles using leaf extract of *Decaschistia crotonifolia* and its antibacterial, antioxidant, and catalytic applications. *Green Chem. Lett. Rev.* **14**(1), 136–151 (2021).
21. Palithya, S. et al. Green synthesis of silver nanoparticles using flower extracts of *Aerva lanata* and their biomedical applications. *Part. Sci. Technol.* **40**(2), 1–13 (2021).
22. Kotakadi, V. S. et al. Dual synthesis of silver and iron oxide nanoparticles from edible green *Amaranthus viridis* and their in vitro antioxidant activity and antimicrobial studies. *Curr. Biotechnol.* **10**(3), 191–203 (2021).
23. Al-Rajhi, A. M. H., Salem, S. S., Alharbi, A. A. & Abdelghany, T. M. Ecofriendly synthesis of silver nanoparticles using Kei-apple (*Dovyalis caffra*) fruit and their efficacy against cancer cells and clinical pathogenic microorganisms. *Arab. J. Chem.* **15**, 103927 (2022).
24. Aref, M. S. & Salem, S. S. Bio-callus synthesis of silver nanoparticles, characterization, and antibacterial activities via *Cinnamomum camphora* callus culture. *Biocatal. Agric. Biotechnol.* **27**, 101689 (2020).
25. Velsankar, K., Parvathy, G., Sankaranarayanan, K., Mohandoss, S. & Sudhahar, S. Green synthesis of silver oxide nanoparticles using *Panicum miliaceum* grains extract for biological applications. *Adv. Powder Technol.* **33**, 103645 (2022).
26. Velsankar, K., Preethi, R., Jeevan Ram, P. S., Ramesh, M. & Sudhahar, S. Evaluations of biosynthesized Ag nanoparticles via *Allium sativum* flower extract in biological applications. *Appl. Nanosci.* **10**, 3675–3691 (2020).
27. World Health Organization. https://www.who.int/breast_cancer.
28. Pushparaj, K. et al. Green synthesis, characterization of silver nanoparticles using aqueous leaf extracts of *Solanum melongena* and in vitro evaluation of antibacterial, pesticidal and anticancer activity in human MDA-MB-231 breast cancer cell lines. *J. King Saud Univ. Sci.* **35**(5), 102663 (2023).

29. Rudrappa, M. et al. Myco-nanofabrication of silver nanoparticles by *Penicillium brasilianum* NP5 and their antimicrobial, photoprotective and anticancer effect on MDA-MB-231 breast cancer cell line. *Antibiotics* **12**(3), 567 (2023).
30. Mohaideen, N. S. H., Ravindranath, K. J. & Srinivasan, H. Targeted cytotoxicity against MDA-MB- 231 triple-negative breast cancer cells with *Borassus flabellifer* haustorium-derived silver nanoparticles: An integrated *in silico* and experimental approach. *Biocatal. Agric. Biotechnol.* **54**, 102952 (2023).
31. Mani, S. T. et al. Green synthesis and characterization of silver nanoparticles from *Eclipta alba* and its activity against triple-negative breast cancer cell line (MDA-MB-231). *Mol. Biotechnol.* https://doi.org/10.1007/s12033-023-00959-w (2023).
32. Gurunathan, S., Han, J. W., Eppakayala, V., Jeyaraj, M. & Kim, J. H. Cytotoxicity of biologically synthesized silver nanoparticles in MDA-MB-231 human breast cancer cells. *Biomed. Res. Int.* https://doi.org/10.1155/2013/535796 (2013).
33. Xu, X., Amraii, S. A., Toushmalani, R. & Almasi, M. Formulation of a modern anti-human breast cancer drug from silver nanoparticles green-synthesized using *Allium saralicum*. *J. Eng. Res.* https://doi.org/10.1016/j.jer.2023.100136 (2023).
34. Darvish, S. et al. Silver nanoparticles: biosynthesis and cytotoxic performance against breast cancer MCF-7 and MDA-MB-231 cell lines. *Nanomed. Res. J.* **7**(1), 83–92 (2022).
35. Tao, L., Chen, X., Sun, J. & Wu, C. Silver nanoparticles achieve cytotoxicity against breast cancer by regulating long-chain noncoding RNA XLOC_006390-mediated pathway. *Toxicol. Res.* **10**(1), 123–133 (2021).
36. Hepokur, C. et al. Silver nanoparticle/capecitabine for breast cancer cell treatment. *Toxicol. Vitro* **61**, 104600 (2019).
37. Abdellatif, A., Abdelfattah, A., Younis, M., Aldalaan, S. & Tawfeek, H. Chitosan-capped silver nanoparticles with potent and selective intrinsic activity against the breast cancer cells. *Nanotechnol. Rev.* **12**(1), 20220546 (2023).
38. Swanner, J. et al. Silver nanoparticles selectively treat triple-negative breast cancer cells without affecting non-malignant breast epithelial cells in vitro and in vivo. *FASEB Bioadv.* **1**(10), 639–660 (2019).
39. Kotakadi, V. S. et al. New generation of bactericidal silver nanoparticles against different antibiotic resistant *Escherichia coli* strains. *Appl. Nanosci.* **5**, 847–855 (2015).
40. Kotakadi, V. S. et al. Ficus fruit-mediated biosynthesis of silver nanoparticles and their antibacterial activity against antibiotic resistant *E. coli* strains. *Curr. Nanosci.* **11**, 527–538 (2015).
41. Bruna, T., Maldonado-Bravo, F., Jara, P. & Caro, N. Silver nanoparticles and their antibacterial applications. *Int. J. Mol. Sci.* **22**(13), 7202 (2021).
42. Haji, S. H., Ali, F. A. & Aka, S. T. H. Synergistic antibacterial activity of silver nanoparticles biosynthesized by carbapenem-resistant gram-negative bacilli. *Sci. Rep.* **12**, 15254 (2022).
43. Crisan, C. M. et al. Review on silver nanoparticles as a novel class of antibacterial solutions. *Appl. Sci.* **11**(3), 1120 (2021).
44. Ipe, D. S., Kumar, P. T. S., Love, R. M. & Hamlet, S. M. Silver nanoparticles at biocompatible dosage synergistically increases bacterial susceptibility to antibiotics. *Front. Microbiol.* **11**, 1074 (2020).
45. Xie, Y. et al. Anti-inflammatory furostanol saponins from the rhizomes of *Smilax china* L. *Steroids* **140**, 70–76 (2018).
46. Shahrajabian, M. H., Sun, W. & Cheng, Q. Tremendous health benefits and clinical aspects of *Smilax china*. *Afr. J. Pharm. Pharmacol.* **13**, 253–258 (2019).
47. Wang, M. et al. *Smilax china* L.: A review of its botany, ethnopharmacology, phytochemistry, pharmacological activities, actual and potential applications. *J. Ethnopharmacol.* **318**, 116992 (2024).
48. Wu, S. T. et al. The active components of *Smilax china* L. against cancer by interfering with the interactions among associated proteins. *J. Func. Foods* **106**, 105591 (2023).
49. Kanwal, L., Ali, S., Rasul, A. & Tahir, H. M. Smilax china root extract as a novel glucose- 6-phosphate dehydrogenase inhibitor for the treatment of hepatocellular carcinoma. *Saudi J. Biol. Sci.* **29**(10), 103400 (2022).
50. Xu, M. et al. Chemical composition, antibacterial properties, and mechanism of *Smilax china* L. polyphenols. *Appl. Microbiol. Biotechnol.* **103**, 9013–9022 (2019).
51. Xu, Y. et al. A new phenylpropanoid-substituted epicatechin from the rhizome of *Smilax china*. *Nat. Product Res.* **37**(20), 3409–3417 (2023).
52. Zhang, Y. et al. The underlying molecular mechanisms involved in traditional Chinese medicine *Smilax china* L. for the treatment of pelvic inflammatory disease. *Evid. Based Complement. Alternat. Med.* **2021**, 5552532. https://doi.org/10.1155/2021/5552532 (2021).
53. Li, X. et al. *Smilax china* L. flavonoid alleviates HFHS-induced inflammation by regulating the gut-liver axis in mice. *Phytomedicine* **95**, 153728 (2022).
54. Joo, J. H. et al. Antimicrobial activity of *Smilax china* L. root extracts against the acne-causing bacterium, cutibacterium acnes, and its active compounds. *Molecules* **27**(23), 8331. https://doi.org/10.3390/molecules27238331 (2022).
55. Feng, H. et al. The flavonoid-enriched extract from the root of *Smilax china* L. inhibits inflammatory responses via the TLR-4-mediated signaling pathway. *J. Ethnopharmacol.* **256**, 112785 (2020).
56. Tian, L. W., Zhang, Z., Long, H. L. & Zhang, Y. J. Steroidal saponins from the genus smilax and their biological activities. *Nat. Prod. Bioprospect.* **7**, 283–298 (2017).
57. Xu, X. X. et al. Development of the general chapters of the Chinese pharmacopoeia 2020 edition: A review. *Chin. Pharmaceut. J.* **15**, 1323–1332 (2018).
58. Li, X., Liu, S., Jin, W., Zhang, W. & Zheng, G. Identification of the constituents of ethyl acetate fraction from *Smilax china* L. and determination of xanthine oxidase inhibitory properties. *Int. J. Mol. Sci.* **24**(6), 5158 (2023).
59. Yang, C., Tang, Q., Liu, J., Zhang, Z. & Liu, W. Preparative isolation and purification of phenolic acids from smilax china by high-speed counter-current chromatography. *Sep. Purif. Technol.* **61**, 474–478 (2008).
60. Sousa, A., Ferreira, I. C. F. R., Barros, L., Bento, A. & Pereira, J. A. Effect of solvent and extraction temperatures on the antioxidant potential of traditional stoned table olives "alcaparras". *Food Sci. Technol.* **41**, 739 (2008).
61. Pick, E. & Mizel, D. Rapid microassays for the measurement of superoxide and hydrogen peroxide production by macrophages in culture using an automatic enzyme immunoassay reader. *J Immunol. Methods* **46**, 211 (1981).
62. Mosmann, T. Rapid colorimetric assay for cellular growth and survival: application to proliferation and cytotoxicity assays. *J. Immunol. Methods* **65**, 55 (1983).
63. Subramanyam, G. K. et al. Green fabrication of silver nanoparticles by leaf extract of *Byttneria Herbacea Roxb* and their promising therapeutic applications and its interesting insightful observations in oral cancer. *Artif. Cell Nanomed. Biotechnol.* **51**(1), 83–94 (2023).
64. Gunti, H., Gaddam, S. A., Nadipi, R. & Kotakadi, V. S. Optical and paper-based dual sensing of Hg 2+ and colorimetric reduction of Cr(VI) by green synthesized silver nanoparticles prepared from the bark extract of *Sweetinia mahagoni* and their promising antimicrobial applications. *Nano Biomed. Eng.* **15**(1), 60–73 (2023).
65. Bruna, T., Maldonado-Bravo, F., Jara, P. & Caro, N. Silver Nanoparticles and Their Antibacterial Applications. *Int J Mol Sci* **22**(13), 7202 (2021).
66. Adil, M. et al. Efficient green silver nanoparticles-antibiotic combinations against antibiotic-resistant bacteria. *AMB Express* **13**, 115 (2023).
67. Adil, M., Khan, T., Aasim, M., Khan, A. A. & Ashraf, M. Evaluation of the antibacterial potential of silver nanoparticles synthesized through the interaction of antibiotic and aqueous callus extract of *Fagonia indica*. *AMB Express* **9**(1), 1–12 (2019).
68. Fayaz, A. M. et al. Biogenic synthesis of silver nanoparticles and their synergistic effect with antibiotics: a study against gram-positive and gram-negative bacteria. *Nanomed. Nanotechnol. Biol. Med.* **6**(1), 103–109 (2010).

69. Vazquez-Muñoz, R. et al. Enhancement of antibiotics antimicrobial activity due to the silver nanoparticles impact on the cell membrane. *PLoS ONE* **14**(11), e0224904 (2019).
70. Thomas, R. et al. Enhanced antimicrobial efficacy of biosynthesized silver nanoparticle based antibiotic conjugates. *Inorg. Chem. Commun.* **117**, 107978 (2020).
71. Fontoura, I., Veriato, T. S., Raniero, L. J. & Castilho, M. L. Analysis of capped silver nanoparticles combined with imipenem against different susceptibility profiles of *Klebsiella pneumonia*. *Antibiotics* **12**, 535 (2023).
72. Deng, H. et al. Mechanistic study of the synergistic antibacterial activity of combined silver nanoparticles and common antibiotics. *Environ. Sci. Technol.* **50**, 8840–8848 (2016).
73. Lopez-Carrizales, M. et al. In vitro synergism of silver nanoparticles with antibiotics as an alternative treatment in multiresistant uropathogens. *Antibiotics* **7**, 1–13 (2018).
74. Tun, W. S. T. et al. The synergistic action of silver nanoparticles and ceftazidime against antibiotic-resistant *Burkholderia pseudomallei*: A modifying treatment. *Process Biochem.* **136**, 351–361 (2024).
75. Muddassir, M. et al. Antibacterial efficacy of silver nanoparticles (AgNPs) against metallo-β-lactamase and extended spectrum β-lactamase producing clinically procured isolates of *Pseudomonas aeruginosa*. *Sci. Rep.* **12**, 20685 (2022).
76. Al-Sheddi, E. S. et al. Anticancer potential of green synthesized silver nanoparticles using extract of *Nepeta deflersiana* against human cervical cancer cells (HeLA). *Bioinorg. Chem. Appl.* **2018**, 9390784 (2018).
77. Muhammad Qasim, N. et al. *Seripheidium quettense* mediated green synthesis of biogenic silver nanoparticles and their theranostic applications. *Green Chem. Lett. Rev.* **12**(3), 310–322 (2019).
78. Pannerselvam, B. et al. Facile synthesis of silver nanoparticles using Asian spider flower and its in vitro cytotoxic activity against human breast carcinoma cells. *Processes* **8**(4), 430 (2020).
79. Banerjee, P. P. et al. *Mentha arvensis* (Linn.)-mediated green silver nanoparticles trigger caspase 9-dependent cell death in MCF7 and MDA-MB-231 cells. *Breast Cancer* **9**, 265–278 (2017).
80. Tabrizi, M. H. et al. Putative mechanism for anticancer properties of Ag-PP (NPs) extract. *IET Nanobiotechnol.* **13**(6), 617–620 (2019).
81. Javed, B., Nadhman, A. & Mashwani, Z. U. R. Phytosynthesis of Ag nanoparticles from *Mentha longifolia*: their structural evaluation and therapeutic potential against HCT116 colon cancer, Leishmanial and bacterial cells. *Appl. Nanosci.* **10**, 3503–3515 (2020).
82. Al-Zaban, M. I., Mahmoud, M. A. & AlHarbi, M. A. Catalytic degradation of methylene blue using silver nanoparticles synthesized by honey. *Saudi J. Biol. Sci.* **28**(3), 2007–2013. https://doi.org/10.1016/j.sjbs.2021.01.003 (2021).
83. Chimentão, R. J., Kirm, I., Medina, F., Rodríguez, X., Cesteros, Y., Salagre, P., & Sueiras, J. E. Different morphologies of silver nanoparticles as catalysts for the selective oxidation of styrene in the gas phase. *Chem. Commun*. (7), 846–847. https://doi.org/10.1039/b400762j (2004).
84. Oliveira, L. S., Franca, A. S., Alves, T. M. & Rocha, S. D. Evaluation of untreated coffee husks as potential biosorbents for treatment of dye contaminated waters. *J. Hazard. Mater.* **155**, 507–512 (2008).
85. Bharathi, D., Diviya Josebin, M. & Vasantharaj, S. Biosynthesis of silver nanoparticles using stem bark extracts of *Diospyros montana* and their antioxidant and antibacterial activities. *J. Nanostruct. Chem.* **8**, 83–92 (2018).
86. Narjala, R. J. et al. Dual degradation of hexavalent chromium (VI) and cotton blue dye by reduced and PVP-capped silver nanoparticles using fruit extract of *Ficus carica*. *Nano Biomed. Eng.* **14**(2), 123–135 (2022).

Acknowledgements

The author VSK is grateful to DST-PURSE Program, sponsored by DST New Delhi, for providing fellowship and SAG grateful to UGC Women PDF Program, sponsored by UGC, New Delhi. and HM thankful to CSIR New Delhi for providing fellowship to research student to carried apart of research work.

Author contributions

Contributions (Authors List) Susmil Aparna Gaddam (SAG), Venkata Subbaiah Kotakadi (VSK), Rajasekar Allagadda (RA), Vasavi T (VT), Siva Gayathri Velakanti (SGV), Srilakshmi Samanchi (SS),Devaraju Thangellamudi (DT),Hema Masarapu (HM), Uma Maheswari P (UMP),Appa Rao Ch (ARCh) and Enyew Amare Zereffa(EAZ) The authors confirm contribution to the paper as follows: SAG and VSK contributed equally to the work Study conception and Design: SAG, VSK, EAZ Data collection: SAG, SS, DT & SGV Experimental: SAG &VSK: Green synthesis and Spectral Characterization;RA &ARCh (Antioxidant studies) VT&UMP (Cytotoxic studies) SGV & HM (Antimicrobial studies) and SAG & DT (Photo-catalytic studies) Analysis and Interpretation of Results: SAG, VSK and EAZ; Draft Manuscript preparation: SAG & VSK, Final Manuscript editing: VSK and EAZ. All authors reviewed the manuscript.

Declarations

Competing interests

The authors declare no competing interests.

Additional information

Correspondence and requests for materials should be addressed to V.S.K. or E.A.Z.